Continental-scale salt tectonics on Mars and the origin of Valles Marineris and associated outflow channels

David R. Montgomery[†]
Sanjoy M. Som
Quaternary Research Center, Department of Earth and Space Sciences, University of Washington, Seattle, Washington 98195-1310, USA
Astrobiology Program, University of Washington, Seattle, Washington 98195-1310, USA

Martin P. A. Jackson
Bureau of Economic Geology, Jackson School of Geosciences, The University of Texas at Austin, Austin, Texas 78713-8924, USA

B. Charlotte Schreiber
Quaternary Research Center, Department of Earth and Space Sciences, University of Washington, Seattle, Washington 98195-1310, USA

Alan R. Gillespie
Quaternary Research Center, Department of Earth and Space Sciences, University of Washington, Seattle, Washington 98195-1310, USA
Astrobiology Program, University of Washington, Seattle, Washington 98195-1310, USA

John B. Adams
Quaternary Research Center, Department of Earth and Space Sciences, University of Washington, Seattle, Washington 98195-1310, USA

ABSTRACT

A synthesis of deformation patterns within and around the Thaumasia Plateau, Mars, points to a new interpretation for regional deformation and the origin of Valles Marineris and associated outflow channels. The morphology of the Thaumasia Plateau is typical of thin-skinned deformation, akin to a "mega-slide," in which extensional deformation in Syria Planum and Noctis Labyrinthus connects via lateral zones of transtension and strike-slip—Claritas Fossae and Valles Marineris—to a broad zone of compressional uplift and shortening defined by truncated craters and thrust faults along the Coprates Rise and Thaumasia Highlands. However, the low regional slope (~1°) results in gravitational body forces that are too small to deform the basaltic lava flows conventionally thought to compose the flanks of the Tharsis volcanic province. Instead, we conclude that geothermal heating and topographic loading of extensive buried deposits of salts and/or mixtures of salts, ice, and basaltic debris would allow for weak detachments and large-scale gravity spreading. We propose that the generally linear chasmata of Valles Marineris reflect extension, collapse, and excavation along fractures radial to Tharsis, either forming or reactivated as part of one lateral margin of the Thaumasia gravity-spreading system. The other, dextral, lateral margin is a massive splay of extensional faults forming the Claritas Fossae, which resembles a trailing extensional imbricate fan. The compressional mountain belt defined by the Coprates Rise and Thaumasia Highlands forms the toe of the "mega-slide." Topographic observations and previous structural analyses reveal evidence for a failed volcanic plume below Syria Planum that could have provided further thermal energy and topographic potential for initiating regional deformation, either intrusively through inflation or extrusively through lava flow and/or ash fall emplacement. Higher heat flow during Noachian time, or geothermal heating due to burial by Tharsis-derived volcanic rocks, would have contributed to flow of salt deposits, as well as formation of groundwater from melting ice and dewatering of hydrous salts. We further propose that connection of overpressured groundwater from aquifers near the base of the detachment through the cryosphere to the martian surface created the outflow channels of Echus, Coprates, and Juventae chasmata at relatively uniform source elevations along the northern margin of the "mega-slide," where regional groundwater flow would have been directed toward the surface. Our hypothesis provides a unifying framework to explain perplexing relationships between the rise of the Tharsis volcanic province, deformation of the Thaumasia Plateau, and the formation of Valles Marineris and associated outflow channels.

Keywords: Mars, salts, sulfates, salt tectonics, Thaumasia, Valles Marineris, gravity spreading, volcanic plume, outflow channels.

INTRODUCTION

Ongoing debate surrounds the relations, if any, between the Tharsis volcanic province, the deformation of the Thaumasia Plateau, the opening of Valles Marineris, and the associated outburst floods (Fig. 1). The wide range of explanations for the formation of Valles Marineris, which exposes the deepest sections through the martian crust, includes structural collapse and/or tectonic rifting based on analogy to terrestrial continental rifts (Table 1). Explanations offered to explain carving of the associated outflow channels include incision by wind, glaciers, debris flows and lava, or catastrophic floods due to thermal response to dike emplacement, discharge from overpressured aquifers, and dewatering of extensive deposits of hydrated salts, as well as explosive depressurization of clathrates and combinations of these mechanisms (Table 2). Although evidence for each explanation accounts for a subset of the observations, no

[†]E-mail: dave@ess.washington.edu

GSA Bulletin; January/February 2009; v. 121; no. 1/2; p. 117–133; doi: 10.1130/B26307.1; 13 figures; 2 tables.

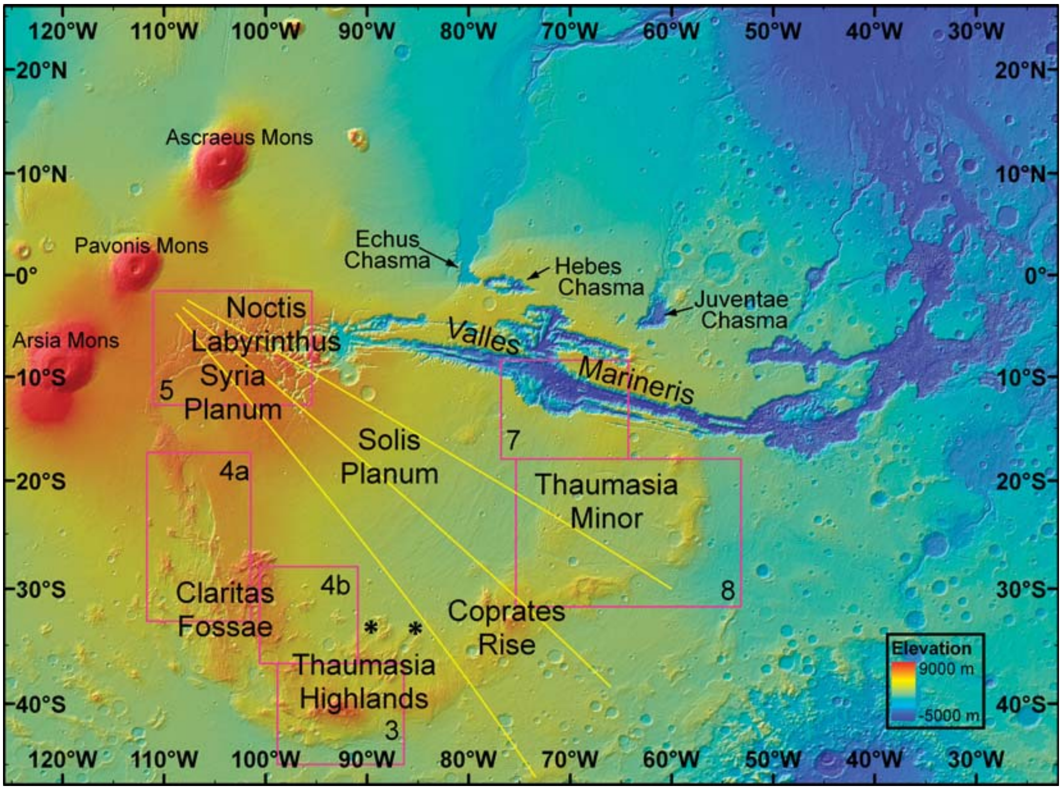

Figure 1. Mars Orbiter Laser Altimeter (MOLA)-derived shaded relief location map of the setting of SE Tharsis, Valles Marineris, and the Thaumasia Plateau, showing place names and the locations of Figures 3–5, 7, and 8, as well as the traces of the topographic profiles shown in Figure 10 (yellow lines). Asterisks show locations of grabens discussed by Grott et al. (2007).

single process or combination of processes has satisfactorily explained connections between the growth of the Tharsis volcanic province, deformation of the Thaumasia Plateau, formation of the Valles Marineris chasmata, and the associated outburst flooding that created Echus, Juventae, and Coprates chasmata.

Discovery of abundant salts by the rover *Opportunity* at Meridiani Planum (Squyres et al., 2004) together with spectral evidence for hydrous sulfates (gypsum and kieserite) associated with layered deposits in Valles Marineris (e.g., Gendrin et al., 2005) from the OMEGA (Observatoire pour la Minéralogie, l'Eau, les Glaces et l'Activité) instrument (Bibring et al., 2006) on board the Mars Express orbiter suggest that salts may be an important component of the layered rocks in the Valles Marineris region, as well as being widespread on Mars. Osterloo et al. (2008) have found spectral evidence of halite, in addition to the hydrous sulfate salts. Evidence that light-toned layered deposits are exposed in the walls of, and therefore predate, the Valles Marineris chasmata (Malin and Edgett, 2000; Montgomery and Gillespie, 2005; Bigot-Cormier and Montgomery, 2007) supports the hypothesis that extensive, thick salt-rich deposits were buried beneath volcanic materials as Tharsis grew from both intrusion and inflation from below and deposition of lava flows, volcanic breccia, and ash from above.

TABLE 1. HYPOTHESES FOR FORMATION OF VALLES MARINERIS

Structural collapse	(Sharp, 1973; Tanaka and Golombek, 1989; Spencer and Fanale, 1990; Schultz, 1998; Schultz and Lin, 2001; Rodriguez et al., 2006)
Tectonic rifting	(Sharp, 1973; Blasius et al., 1977; Frey, 1979; Masson, 1977, 1985; Schoenfield, 1979; Anderson and Grimm, 1998; Schultz, 1991, 1995; Peulvast and Masson, 1993, Mége and Masson, 1996b; Peulvast et al., 2001)
Combination of mechanisms	(Lucchitta et al., 1992; Schultz, 1998)

TABLE 2. HYPOTHESES FOR FORMATION OF MARTIAN OUTFLOW CHANNELS

Thermal response to dike emplacement	(McKenzie and Nimmo, 1999)
Erosion by catastrophic floods	(Baker and Milton, 1974; Robinson and Tanaka, 1990; Komatsu and Baker, 1997)
Discharge from overpressured aquifers	(Carr, 1979)
Dewatering of voluminous hydrated salts	(Montgomery and Gillespie, 2005)
Explosive depressurization of clathrates	(Milton, 1974; Lambert and Chamberlain, 1978; Hoffman, 2000)
Incision by wind	(Cutts and Blasius, 1981)
Incision by glaciers	(Lucchitta et al., 1981)
Incision by lava flows	(Leverington, 2004)
Incision by debris flows	(Tanaka, 1999)
Incision by CO_2-supported debris flows	(Hoffman, 2001)

Montgomery and Gillespie (2005) hypothesized that heating and dewatering of extensive buried evaporite deposits generated the great discharges that carved channels as outflows from Valles Marineris and vicinity. Elaborating upon that idea to propose a single mechanism to form Valles Marineris, Noctis Labyrinthus, and the compressional highlands ringing the Thaumasia Plateau, we draw on prior research, analyses of Mars Orbiter Laser Altimeter (MOLA; Zuber et al., 1992) topography, and interpretation of Thermal Emission Imaging System (THEMIS; Christensen et al., 2004) and Mars Orbiter Camera (MOC; Malin et al., 1991) images to propose regional deformation moving down a gentle topographic slope. This gravity-driven deformation produced a linked extensional-contractional system detached on flowing salts or salt-rich deposits heated from below and loaded from above by burial during the rise of Tharsis and Syria Planum. Within and at the toe of the deforming region, fractures connected an overpressured, confined aquifer below the cryosphere to the surface and triggered outburst floods. Such a large-scale detachment, or "megaslide," explains otherwise perplexing aspects of relations between the growth of Tharsis, deformation of the Thaumasia Plateau, and the origin of Valles Marineris and its outburst floods.

BACKGROUND

Despite the wide range of proposed explanations for the formation of Valles Marineris, few attempts have been made to link its growth to the regional setting and evolution of the Thaumasia Plateau beyond the general recognition of the volcanic province of Tharsis as a logical source of both heat and topographic potential. The Thaumasia Plateau extends almost 3000 km across and rises >4 km above the surrounding plains. It is now generally accepted that formation of the Thaumasia Plateau involved: (1) increased mass from intrusion and extrusion of volcanic rocks; and (2) contractional deformation from tectonic activity (Schultz and Tanaka, 1994). However, the mechanisms responsible for the deformation of the Thaumasia Plateau are still debated. For example, Dohm and Tanaka (1999) attributed formation of the plateau to deformation comparable to intracontinental plateaus like the Rocky Mountains fold-and-thrust belts. Anguita et al. (2001) proposed that the Thaumasia Plateau was an independent lithospheric block that buckled in the Late Noachian–Early Hesperian under E-W compression, forming the Valles Marineris chasmata by transtensional deformation (inferred by them to be dextral) along the northern margin of the Thaumasia block. They also concluded that deformation of the Thaumasia Plateau involved an early thick-skinned event in the Late Noachian–Early Hesperian (ca. 3.6 Ga) and later thin-skinned deformation in the Amazonian (<3 Ga). More recently, Anguita et al. (2006) reexamined tectonic structures at Thaumasia Plateau and neighboring Daedalia Planum and Aonia Planum, and proposed that these areas formed part of a larger Noachian orogen.

Perhaps the most globally prominent of martian landforms—other than large volcanoes and impact basins—is Valles Marineris, an immense, remarkably linear, canyon system of distinct troughs that extends more than 1500 km along the northern margin of the Thaumasia Plateau. Conventional explanations favoring rifting have focused on the linearity of individual troughs comprising Valles Marineris and on prominent fault scarps in many of the chasmata as evidence for a tectonic origin (e.g., Frey, 1979; Peulvast and Masson, 1993; Peulvast et al., 2001). Conversely, those inferring structural collapse typically point to the closed depression of Hebes Chasma as compelling evidence for removal of subsurface support (e.g., Spencer and Fanale, 1990; Schultz, 1998).

The stratigraphy of the region has also been debated, in particular whether the layered deposits exposed in Valles Marineris formed before or after the present chasmata. Some hold that the layered deposits formed in lakes (e.g., Nedell et al., 1987; Komatsu et al., 1993; Lucchitta et al., 1994; Quantin et al., 2005; Dromart et al., 2007) or as sub-ice volcanoes (Chapman and Tanaka, 2001) within Valles Marineris, and thus that the layered deposits are younger than the chasmata walls. These walls are widely thought to consist of basaltic lava flows, based on local exposures of layering extending through the entire section (McEwen et al., 1999). Although contacts between the layered materials and wall rocks are obscure throughout most of the Valles Marineris chasmata, Malin and Edgett (2000) reported that MOC images reveal layered deposits within Valles Marineris that extend, in places, beneath the darker wall-forming material, and thus predate the chasmata there. Williams et al. (2003) showed that layering in the wall rock extends deeper in the western parts than in the eastern parts of the main trough of Valles Marineris, and proposed that both extrusive and intrusive magmatism formed the layering. However, examination of additional MOC images of areas where layered deposits are exposed in Melas Chasma (Montgomery and Gillespie, 2005) and Juventae Chasma (Catling et al., 2006) also show light-toned layered formations extending under darker rocks that form the canyon walls. Montgomery and Gillespie (2005) further posited that Tharsis-related volcanism buried extensive deposits of hydrous salts. Bigot-Cormier and Montgomery (2007) reported additional evidence for a contact between wall-forming material and an underlying weaker layer in the walls of Candor, Ophir, and Melas chasmata within Valles Marineris. Together these observations challenge the widely held view that the crust exposed in the walls of the Valles Marineris chasmata consists entirely of stacked basalt flows, even if this may be so in some locations (e.g., McEwen et al., 1999).

An active cryosphere in the martian regolith has long been recognized (Sharp, 1973), but recent discovery of extensive salt deposits on Mars (Squyres et al., 2004; Gendrin et al., 2005; Osterloo et al., 2008) suggests that much of the martian crust is composed of three end-member materials: (1) basaltic ash, flows, and rubble, (2) liquid water or ice, and (3) salts and hydrated salts. Hence, the different physical properties of exposed or buried salt and salt-rich deposits provide a potentially underappreciated third component that could influence martian landforms. In particular, extensive deposits of buried salts, or salt-cemented deposits, could provide both subsurface ductile layers and sources for diapiric or extrusive salt tectonics. In contrast to both liquid water and ice, which are unstable under ambient surface conditions and are lost over time, many salts are stable at martian surface conditions but may dewater (e.g., Montgomery and Gillespie, 2005) or readily deform viscously (e.g., Schreiber and Helman, 2005). Saline deposits on Mars may include both chloride and sulfate salts, and perhaps other compounds. At least three potential mechanisms could account for such deposits: (1) precipitation at the ground surface due to evaporative concentration, such as within a shallow or ephemeral lake; (2) subsurface precipitation as cements and displacive salts within porous sediments through evaporation, brine cooling, and/or brine mixing; and (3) precipitation from pressure release of salt-saturated supercritical waters ("outsalting" in the sense of Hovland et al., 2006). Although ice could persist near the surface of Mars if buried by dust or rubble (Mellon et al., 1997), and the depth to the martian cryosphere varies latitudinally, the origin, extent, and geomorphic influence of a martian "halosphere" remains to be established. In this context, a ternary diagram with the end-members referred to above provides a formal way to conceptualize the influence of the three primary landscape-forming materials on Mars.

OBSERVATIONS

Spectroscopic and Stratigraphic Evidence for Salts Exposed in Valles Marineris

Gendrin et al. (2005) identified sulfate salts from OMEGA spectra of light-toned layered deposits in Ius, Hebes, Juventae, and Capri chasmata. It is not yet clear whether all light-toned deposits exposed in the Valles Marineris chasmata can be interpreted as containing salts. The absence of salt spectra for some light-toned deposits may be due to dust cover, masking by other spectral components, or concentrations of salt minerals below the OMEGA detection threshold. Other possibly common salts such as halite do not have diagnostic spectral features in the near-infrared wavelength range sampled by OMEGA. Although salts might be expected to have higher albedos than surrounding materials, albedo is not a reliable indicator of composition. Salts readily darken when they contain even trace amounts of optically absorbing components such as metal oxides and sulfides or organic compounds (e.g., Talbot and Aftabi, 2004) or when they are subjected to ionizing radiation. For example, dark gypsum dunes have been identified in the north-polar region of Mars (Langevin et al., 2005). Even though the proportion of salt minerals in the Valles Marineris chasmata is not known, the spectroscopic evidence confirms that locally some layers are salt rich and may even be pure enough to fall near the salt end-member in our proposed ternary diagram.

If salts are concentrated in the light-toned layered deposits, evidence cited above indicates that they occur over a wide range of stratigraphic positions throughout the Valles Marineris chasmata from the rims of chasmata to the base of cliff walls 6–8 km below (Malin and Edgett, 2000; Montgomery and Gillespie, 2005; Bigot-Cormier and Montgomery, 2007). However, light-toned layered rocks are not restricted to the sides and floors of the chasmata. MOC images at Ius and Candor chasmata within Valles Marineris, as well as Juventae Chasma (Catling et al., 2006), show them on the highland plains (at Ius and west Candor the light-toned layered deposits rim the chasmata). Other images show them in crater floors and highland plains far from the chasmata. Hence, potential salt-rich deposits appear to span the extent of Valles Marineris, extend beneath the surrounding plains, and be locally concentrated in the martian crust (Kargel et al., 2007). Also spectral detection of halite shows it to be widely distributed (Osterloo et al., 2008).

Structural and Geomorphological Analyses of MOLA Data

In contrast to ongoing debate about the stratigraphy, there appears to be less debate over the structural geology around Tharsis and the Thaumasia Plateau. Consistent styles of deformation in different areas around the Thaumasia Plateau indicate coherent local and regional spatial patterns. Extension in Syria Planum and Noctis Labyrinthus in the NW transitions to shortening along the Coprates Rise and Thaumasia Highlands in the SE. In addition, models of stress patterns resulting from growth of the Tharsis volcanic province describe the observed pattern of radial tension cracks and grabens, including the general alignment of the chasmata composing Valles Marineris (Banerdt et al., 1982; Mége and Masson, 1996a).

Structural evidence around Tharsis points to early radial fracturing followed by uplift along the Coprates Rise and Thaumasia Highlands and shortening in the form of well-developed wrinkle ridges on the Thaumasia Plateau (Anderson et al., 2001; Borraccini et al., 2007). In particular, Schultz and Tanaka (1994) mapped deformation at two distinct scales within and on the margins of the Thaumasia Plateau. They concluded that a well-defined zone of shortening extending from the Coprates Rise (60°W 15°S) along the Thaumasia Highlands to the western edge of Solis Planum (110°W 30°S) resulted from buckling and thrust faulting that drove 2–4 km of uplift of Noachian and perhaps Early Hesperian units. Schultz and Tanaka (1994) held that the Thaumasia Plateau was pushed over the adjacent foreland, in a manner that Dohm and Tanaka (1999) later interpreted to be consistent with crustal underplating.

The distribution of thrust faults, normal faults, and wrinkle ridges were mapped onto a grayscale MOLA, shaded-relief base map, drawing on a MOLA-registered THEMIS global map (http://jmars.asu.edu/data) and using infrared, elevation, and visible data (Fig. 2). Each mapped line represents two conjugate faults because normal fault traces are the width of a typical graben. Only a few faults are shown where they are densely spaced; we did not try to map all apparent fractures but instead chose to map illustrative features where we had high interpretive confidence. Wrinkle-ridge traces were mapped along the middle of both sharp-crested ridges and flat-crested ridges, either of which may have faults on one or both sides. Probable thrust traces were inferred mostly from truncated craters or scarp morphology.

Thrust Faults

We traced structures visible on a MOLA-derived base map (Fig. 3), as revealed by truncated craters and surficial lobate scarps, indicative of shortening. A map of the compressional features along the base of the Coprates Rise and the Thaumasia Highlands (Schultz and Tanaka, 1994) is extended in Figure 3, using the topographic data and higher-resolution images now available and confirms their pattern of compressional deformation along the southern edge of the Thaumasia Highlands and Coprates Rise. However, this new mapping further reveals that deformation is distributed on several sets of thrust faults along the fault zone, an observation consistent with the toe of a major fold-and-thrust belt. Here the axial trace of the frontal anticline is mapped, although its position is somewhat subjective because the anticline is gentle and broad.

Grabens

The western border of the Thaumasia Plateau is marked by the distinctive aligned grabens of Claritas Fossae, which are consistent with both significant extension and dextral shear (Masson, 1980). Based on mapped fault patterns, Plescia and Saunders (1982) concluded that extension in northern Syria Planum followed deformation in the Thaumasia Highlands. Grott et al. (2007) described two subparallel grabens in the Thaumasia Highlands (extending SSW from locations indicated by asterisks in Fig. 1), and through structural analyses and numerical modeling, determined that these features reflected strain localization in weak zones (which they believed to be volcanic in origin). Crater counting led Grott et al. (2005) to date extension as prior to 3.5 Ga, comparable to the Late Noachian–Early Hesperian formation of Valles Marineris. Based on graben margin flexure, Grott et al. (2005) also estimated that the elastic thickness of the Thaumasia Highlands was 10–13 km and that heat flow there, at least during the Late Noachian–Early Hesperian, was higher than in other areas of Mars.

East and north of these grabens, a continuous zone of extension reaches from Syria Planum to Noctis Labyrinthus at the western end of Valles Marineris. Tanaka and Davis (1988) documented normal faulting and extension in Syria Planum on the NW end of the Thaumasia Plateau and argued that closely spaced faults in Noctis Labyrinthus and Claritas Fossae evolved at the same time. Based on graben widths, they calculated that the faulted thickness ranged from 0.5 to 4.5 km. Arguing in favor of response to local uplift of Syria Planum rather than Tharsis-wide loading, they inferred radial fracturing in response to local mantle diapirism and uplift. Later, concentric faulting was attributed to crustal relaxation, and perhaps magma withdrawal as lava flows erupted onto Syria Planum. They further inferred that the troughs and grabens of Noctis Labyrinthus were roughly coeval with the formation of Valles Marineris.

Our mapping of extensional grabens on the Thaumasia Plateau shows two distinctive areas and styles of deformation: Claritas Fossae and Noctis Labyrinthus. The linear grabens in the western margin in Claritas Fossae resemble the lateral margin of a gravity-spreading fan. Dextral deformation at Claritas Fossae is indicated by (1) a splay geometry resembling a trailing extensional imbricate fan (Fig. 2), (2) apparent R shears and P shears on the western margin (Fig. 4A), (3) left-stepping, en echelon fault arrays farther east (Fig. 4B), and (4) curvature of wrinkle ridges near this boundary (Fig. 2), as described below.

The polygonal pattern of extensional grabens in Noctis Labyrinthus (Fig. 5) reflects two generations and orientations of faults; older NNE-striking grabens and the younger concentric fracture set ringing Syria Planum and curving into Valles Marineris. The rim of Syria Planum remains high, arched, and extended by the concentric pattern of normal faults.

Wrinkle Ridges

The complex pattern of wrinkle ridges on Solis Planum provides additional evidence for the structural style (Schultz and Tanaka, 1994). Schultz (1989), for example, reported both left-lateral and right-lateral faulting that predated or overlapped the formation of wrinkle ridges south of Valles Marineris. Mueller and Golombek (2004) extensively discuss prior work on martian wrinkle ridges. Generally, these features are thought to form transverse to the direction of motion as the surficial signature of blind thrusts resulting from regional shortening, even though there has been substantial disagreement as to whether or not deformation was deeply rooted (e.g., Zuber and Aist, 1990; Tanaka et al., 1991; Golombek et al., 2001; Montesi and Zuber, 2003) or thin-skinned (e.g., Mangold et al., 1998; Okubo and Schultz, 2004; Anguita et al., 2006).

Mangold et al. (1998) investigated whether wrinkle ridges formed by deep thrusting, buckling of lava plains, or thrusting on shallow décollements. They showed that structural relations between wrinkle ridges and faulted craters were inconsistent with both buckling and deeply rooted faulting, but were consistent with shallow-rooted thrusting. They further argued that the décollement depth was not related to the thickness of lava flows, but instead to the depth to ground ice, which deforms ductilely and therefore can provide a detachment surface. Based on a simple geometric model for the depth to a décollement for a compressional pop-up structure, Mangold et al. (1998) estimated the depth to the detachment beneath wrinkle ridges elsewhere on Mars to range from 1 to almost 4 km.

Okubo and Schultz (2004) analyzed the morphology of wrinkle ridges in the western hemisphere of Mars. From maps of backthrusts, they determined that the crust beneath Solis and Thaumasia plana varies in strength, as would arise from interstratified weak layers or reservoirs of near-surface volatiles (e.g., ice). In contrast, most areas outside the Thaumasia Plateau lacked backthrusts, indicating stronger detachments having more frictional resistance. Okubo and Schultz (2004) predicted that the backthrusts associated with wrinkle ridges in the Thaumasia Plateau indicated weak layers in the upper 2–5 km. They further invoked a primary thrust beneath the Solis Planum wrinkle ridges at >10 km depth.

Anguita et al. (2006) noted that the spacing of wrinkle ridges in Nectaris Fossae, the easternmost part of the Thaumasia Plateau, decreases from ~60 km to <20 km in the easternmost

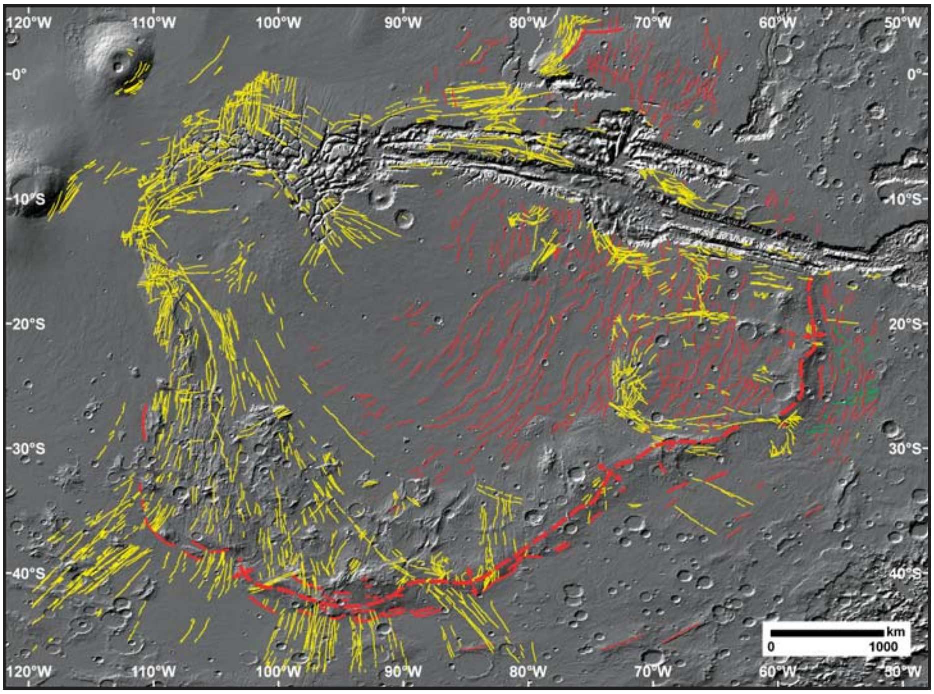

Figure 2. Shaded-relief map of the Thaumasia Plateau (Mars Orbiter Laser Altimeter [MOLA] base) showing mapped distribution of thrust faults (thick red), normal faults (yellow), wrinkle ridges (thin red), and dikes (green) on the Thaumasia Plateau and immediate vicinity.

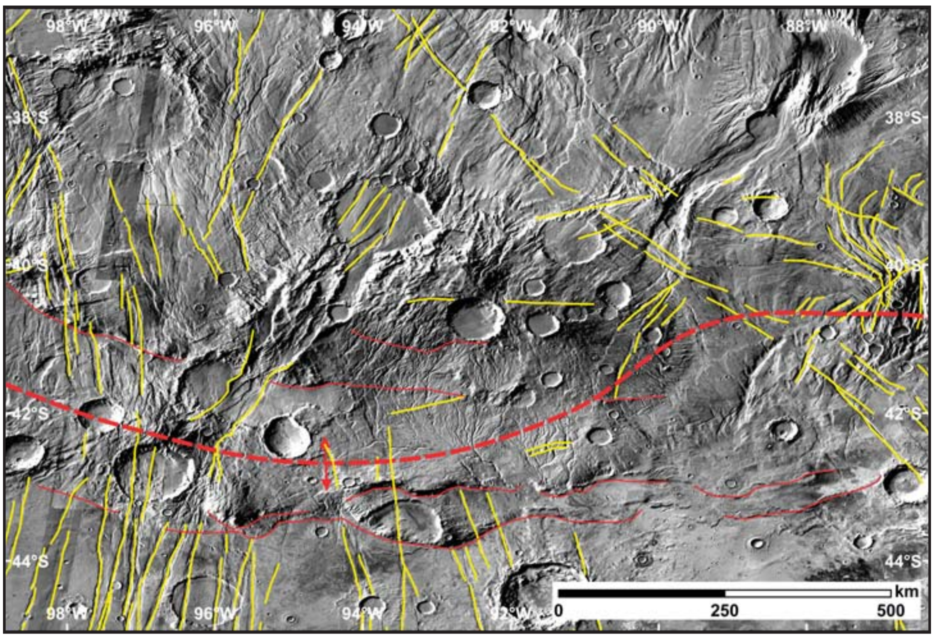

Figure 3. Shaded-relief map of the Thaumasia Highlands (Thermal Emission Imaging System infrared [THEMIS IR] base) showing the distribution of normal faults (yellow) and thrust faults (thin red), trace of frontal anticlinal (thick red), and truncated craters along the southern edge of the Thaumasia Plateau.

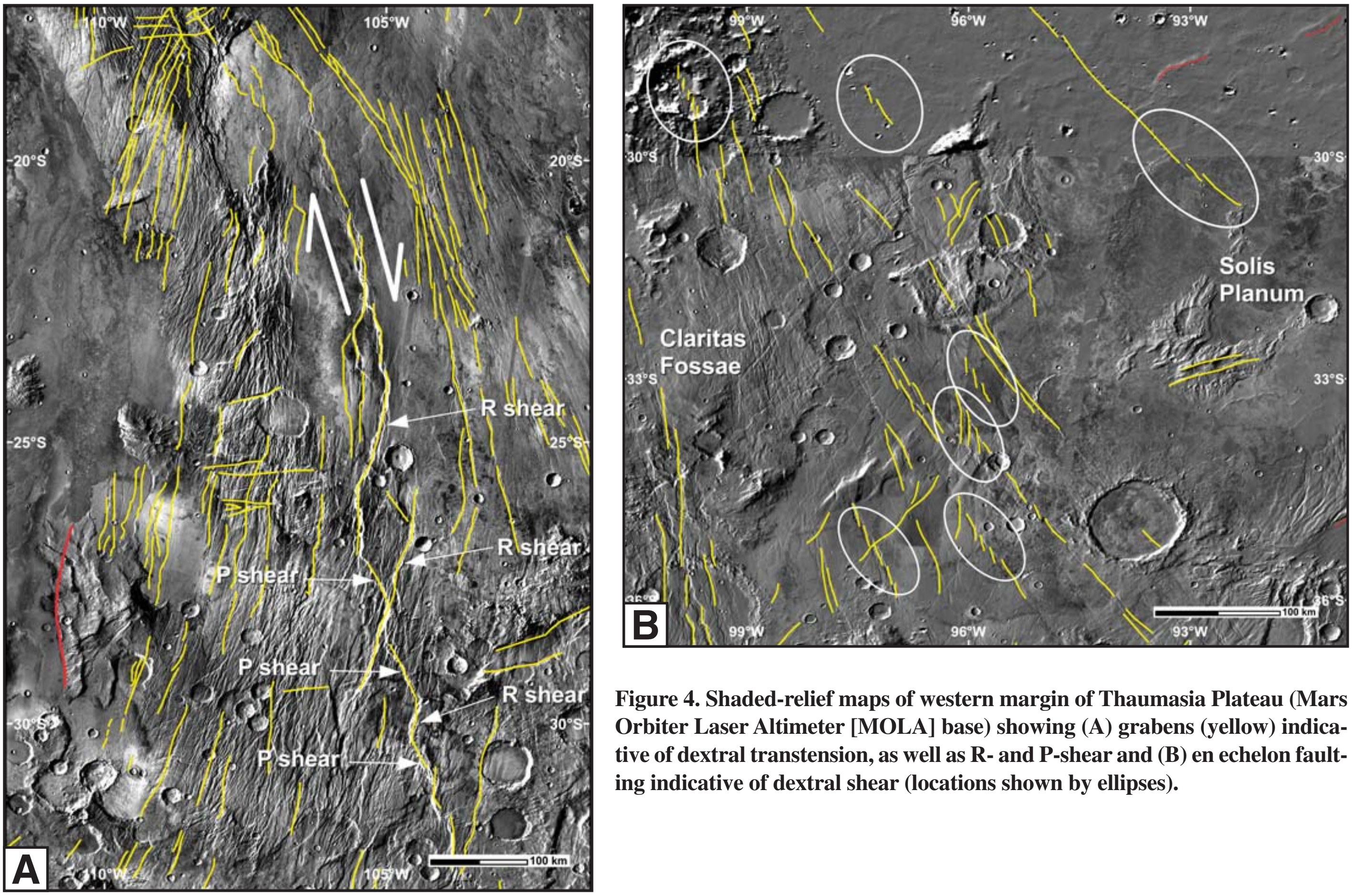

Figure 4. Shaded-relief maps of western margin of Thaumasia Plateau (Mars Orbiter Laser Altimeter [MOLA] base) showing (A) grabens (yellow) indicative of dextral transtension, as well as R- and P-shear and (B) en echelon faulting indicative of dextral shear (locations shown by ellipses).

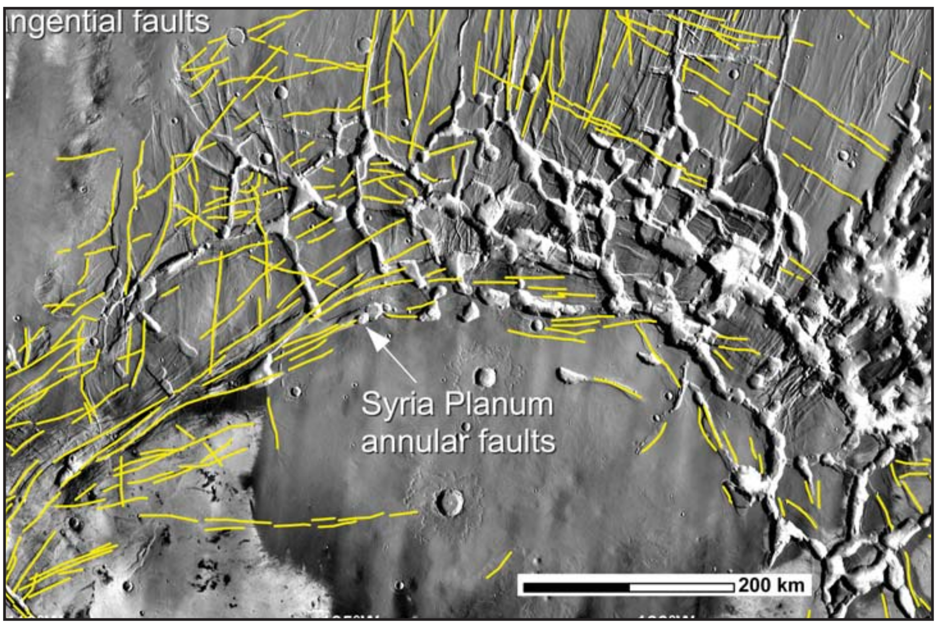

Figure 5. Shaded-relief map of Syria Planum and Noctis Labyrinthus (Thermal Emission Imaging System infrared [THEMIS IR] base) showing intersecting sets of N-S–striking and annular normal faults (yellow) that form a regional polygonal chaos.

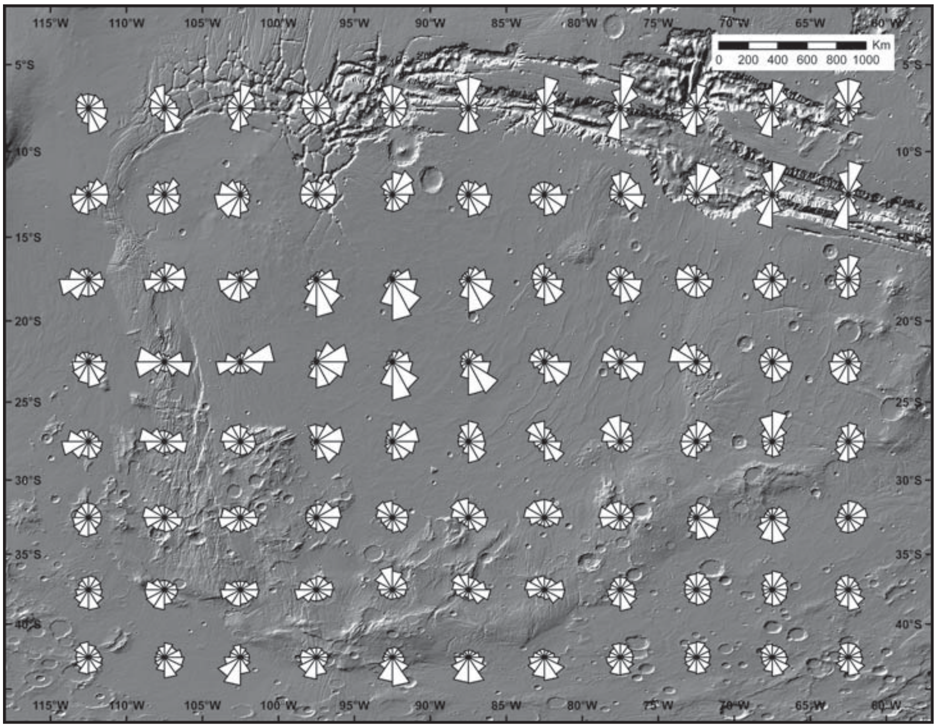

Figure 6. Rose-diagram map showing the distribution of aspects for topography steeper than 5° for a 5° × 5° grid across the Thaumasia Plateau.

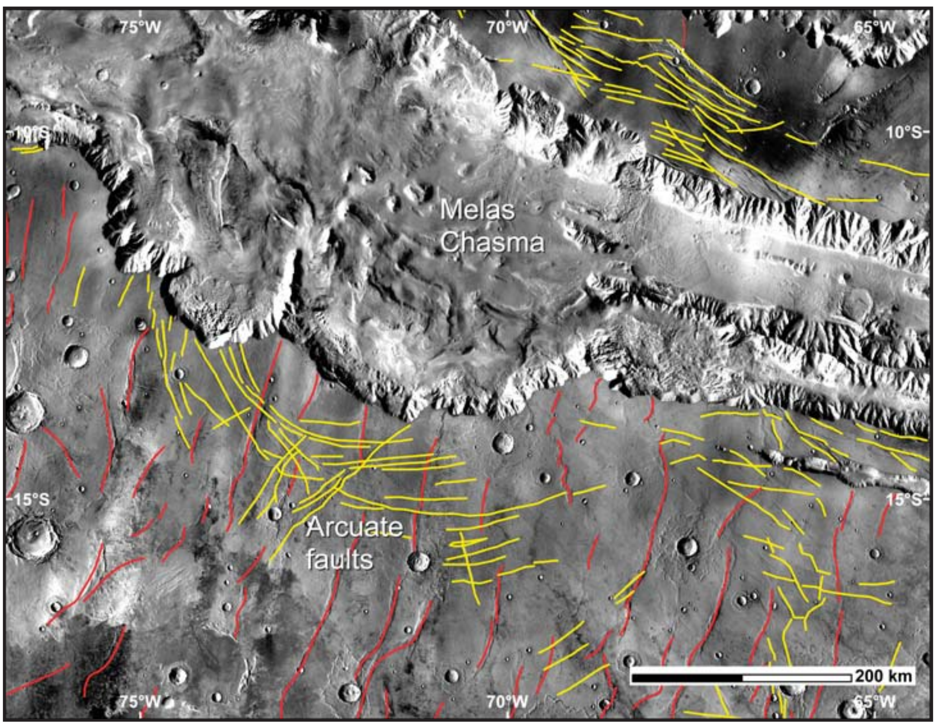

Figure 7. Shaded-relief map of Melas Chasma (Thermal Emission Imaging System infrared [THEMIS IR] base) showing wrinkle-ridge axes (red) and grabens (yellow), indicating extensional unloading revealed by arcuate grabens on the S side and stepped grabens on the N side of the chasma.

margin of the highlands. The inferred depth to the detachment beneath the Thaumasia Plateau decreases from 8 to 15 km under the main plateau to 2–6 km beneath its easternmost edge. They interpreted this decrease to indicate that the décollement beneath the eastern edge of the Thaumasia Plateau dips to the west at 0.6°–3.7°, a range of dips comparable to detachments beneath terrestrial thrust wedges.

Vectors orthogonal to the wrinkle ridges are used to map the flow patterns that formed them. Dividing the Thaumasia Plateau into a 5° × 5° grid (i.e., a 300-km grid at the equator that reduces to a 221-km grid at the southern end of the study area) allows compiling the distribution of aspects (i.e., directions normal to the ground surface) for slopes steeper than 5°. For each grid cell so defined, a rose diagram can show the distribution of vectors orthogonal to the dominant wrinkle-ridge orientation. The resulting map pattern reveals downslope and outward tectonic transport across much of the plateau (Fig. 6). On the western and eastern margins of the plateau, the rose diagrams indicate extension caused by outward spreading, whereas in Solis Planum the rose diagrams show NW-SE shortening. On the plains beyond the Thaumasia Plateau, the rose diagrams indicate no directional bias to slopes >5°.

In addition, we note that the wrinkle-ridge curvature at the SW margin of the Thaumasia Plateau is compatible with dextral shear, based on physical modeling of gravity spreading on salt structures (e.g., Vendeville, 2005), which shows that extensional structures curve downdip near sidewalls, whereas contractional structures curve updip near sidewalls.

Canyon Wall Unloading

The pattern of younger chasmata-parallel fault scarps on the edges of Valles Marineris provides further evidence for mobility on layers at depth after the chasmata opened. In particular, the pattern of grabens bordering Melas Chasma indicates lateral extension due to canyon-wall unloading (Fig. 7). The normal faults cut the wrinkle ridges, so Melas Chasma must have widened after the wrinkle ridges formed. Similarly, the projection of some normal faults into the present canyon walls shows that the canyon widened after extension began. Particularly telling are arcuate scarps set back from and subparallel to the arcuate southern edge of Melas Chasma in the heart of Valles Marineris. The strikes of these fractures indicate that they postdate formation of the chasma and hence reveal further extension across a broad area toward the free face of the chasma walls. Similarly, grabens on the northern side of Melas Chasma record post-chasmata normal faulting indicative of broad deformation and movement of the surrounding upland toward the chasma walls.

Thaumasia Minor

The mapped fault pattern also reveals a second gravity-spreading system, which we call Thaumasia Minor, contained within, but moving ahead of the Thaumasia Plateau (Fig. 8). The western boundary of this smaller feature is extensional; the eastern boundary is a major contractional frontal anticline; the northern boundary is transtensional in the NW but may become transpressional to the E; and the southern boundary is transtensional. A large jog in the frontal anticline coincides with the front of Thaumasia Minor, suggesting an offset continuation of the Thaumasia Highlands–Coprates Rise anticline. In addition, a concentration of wrinkle ridges in the frontal plain indicates increased compression in this part of the foreland, where additional straight ridges interpreted to be dikes of some sort cut the foreland plain. These dike-like features are roughly perpendicular to the frontal scarp and also occur locally within Thaumasia Minor. Dikes tend to be emplaced parallel to the principal stress, which would have been parallel to the transport direction of Thaumasia Minor. Some inferred dikes strike NW or NE; they are oblique to wrinkle ridges and offset them, indicating that dikes formed after the onset of shortening that created the wrinkle ridges. These oblique straight ridges may be conjugate strike-slip faults dilated by dike injection. They suggest more slip than represented solely by the Thaumasia Highlands–Coprates Rise anticline.

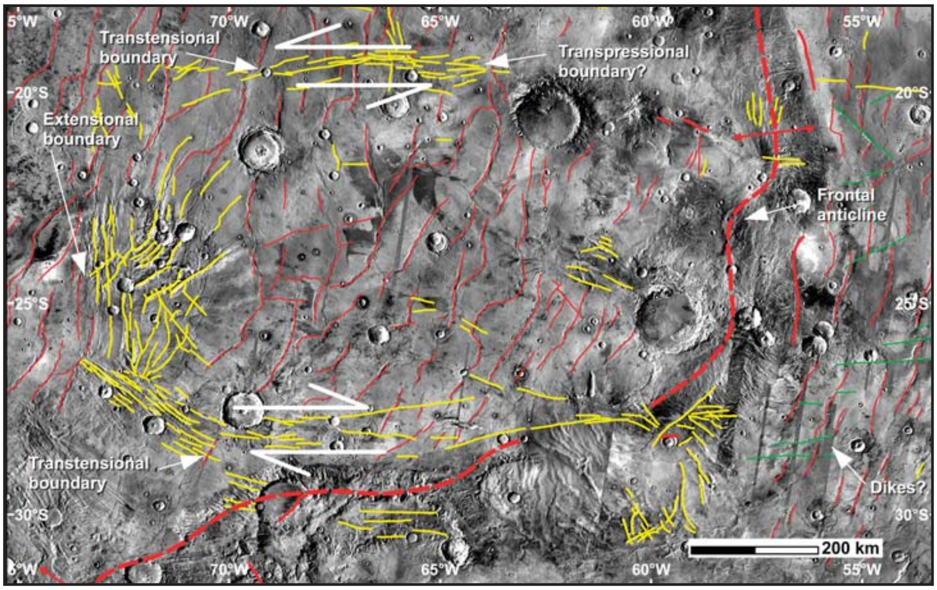

Figure 8. Shaded-relief map of Thaumasia Minor (Thermal Emission Imaging System infrared [THEMIS IR] base) showing structural features: thrust faults (thick red), normal faults (yellow), wrinkle-ridge (thin red), and inferred dikes (green).

INTERPRETATION OF COMPOSITE DEFORMATION

The map pattern of these different styles of deformation around the Thaumasia Plateau strikingly resembles an immense landslide (Fig. 9). Extension around Syria Planum and Noctis Labyrinthus corresponds to an incipient headscarp. Dextral transtension along the western margin of the plateau and suspected sinistral and extensional offset in and around Valles Marineris define the lateral extent of deformation. Contraction and uplift along the Thaumasia Highlands and Coprates Rise correspond to a landslide toe connecting the zones of lateral extension and shear to complete the boundary around the Thaumasia Plateau. A notable aspect of the plateau is that it widens markedly downslope, as discussed further below.

We interpret the composite deformation pattern as indicating three linked gravity-spreading

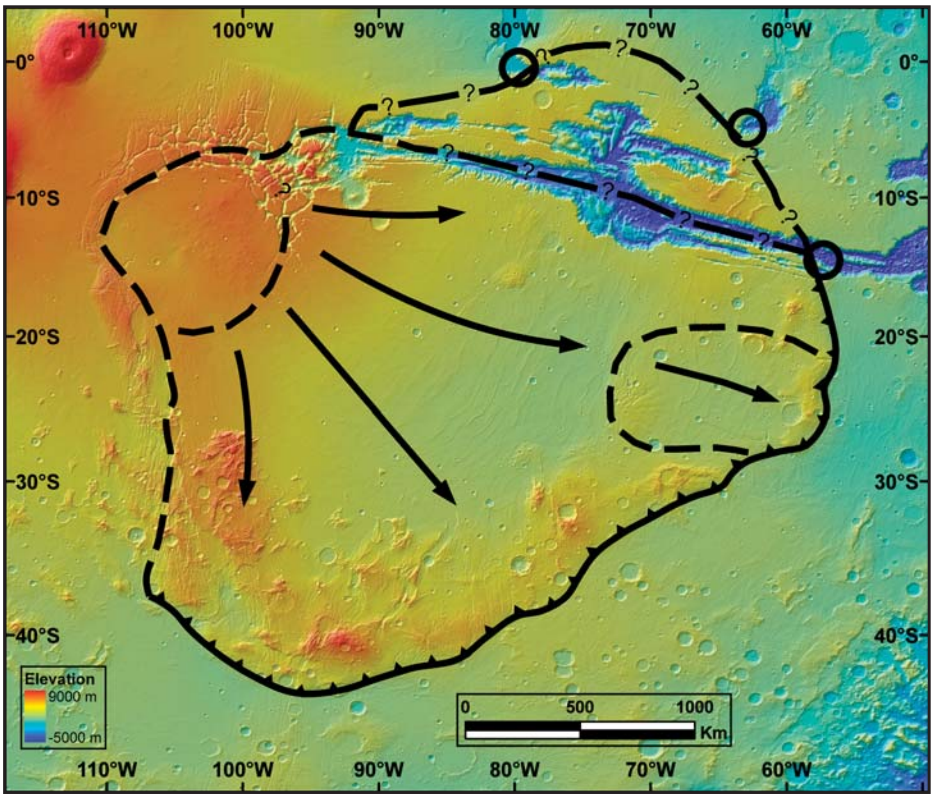

Figure 9. Shaded-relief map of the Thaumasia Plateau (Thermal Emission Imaging System infrared [THEMIS IR] base) showing the broad-scale, inferred sense of translation during gravity spreading, and the boundaries of “microplates” (dashed lines) and outflow channels (open circles).

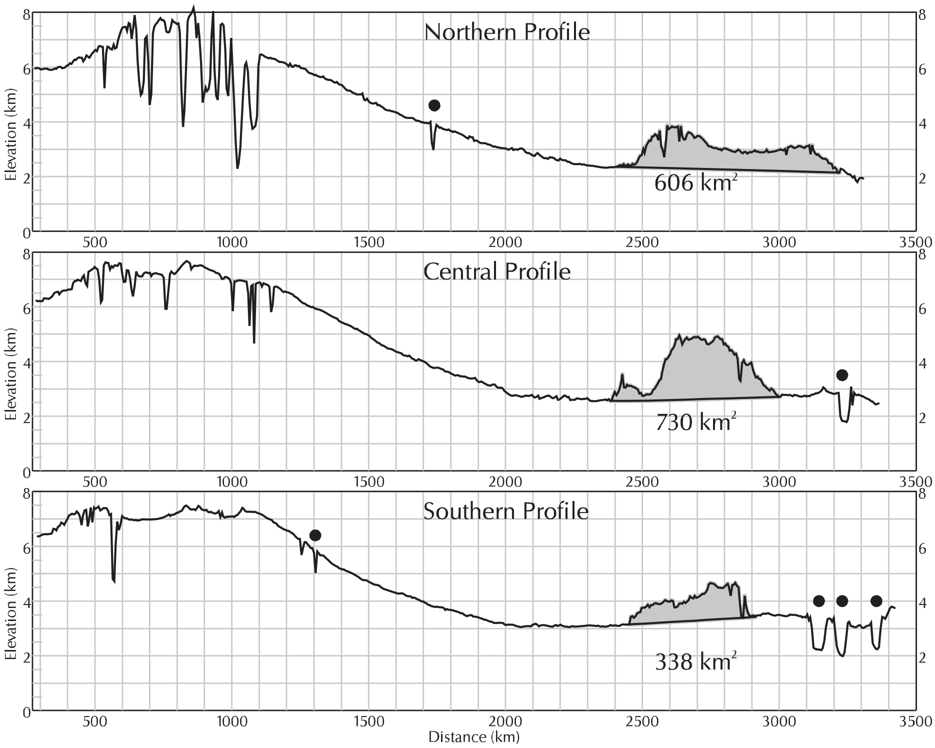

Figure 10. Longitudinal profiles across Thaumasia Plateau through Solis Planum (locations shown in Fig. 1). Vertical exaggeration is 100:1. Shaded area is the "excess area" of the Coprates Rise–Thaumasia Highlands projecting above the regional elevation trend. Dots mark locations of craters intersected by the profiles.

systems: the larger Thaumasia Plateau, and two smaller "plates" having the same sense of tectonic transport. The large Thaumasia Plateau moved ESE as a gravity-spreading system off a dome centered on Syria Planum, now apparently collapsed by volcanic extrusion and/or dewatering of hydrous salts. The two smaller "plates" moved by slightly different amounts, causing extensional faults to separate them from the main Thaumasia Plateau: Syria Planum lagged behind, and the Thaumasia Minor "plate" moved ahead. The plain in the foreland of Thaumasia Minor is also different from flanking areas of the same plain: it contains more wrinkle ridges, and appears to be cut by dike swarms. Nearly all frontal structures (strike-slip faults, thrusts, wrinkle ridges, dikes, and the frontal anticline) have the same inferred paleostress directions, signifying compression from the west.

In this context, there are at least two possible origins for the frontal anticline bounding the Thaumasia Plateau on the SE and E. One possibility is that this is merely a deformation front where gravity spreading ground to a halt but could have advanced farther if the gravity drive had been stronger or the rocks weaker. Alternatively, the frontal anticline marks a stratigraphic limit of the detachment. Similarly, in some terrestrial evaporite basins the frontal shortening structures coincide exactly with the limits of the evaporite basin (e.g., Perdido and Mississippi Fan fold belts in Gulf of Mexico; Lower Congo Basin of offshore Angola; Ebro Basin in Spain; and Melville Island fold belt in Arctic Canada).

The SW margin of the Thaumasia spreading system is well defined as a zone of dextral shear by three consistent criteria: (1) en echelon fault relays, (2) a fault splay (a trailing extensional imbricate fan) forming the Claritas Fossae structural province, and (3) curvature of wrinkle ridges and normal faults. Failing to support (or contradict) either of the conflicting interpretations of Anguita et al. (2001) and Borraccini et al. (2007), we found no kinematic indicators for the sense of shear along the northern boundary of Thaumasia, which we assume to involve sinistral deformation because of the downslope direction of gravity spreading. However, evidence for sinistral shear on the northern margin of the Thaumasia Plateau could have been eroded during excavation of Valles Marineris because the troughs have widened significantly since their initial excavation (e.g., Schultz, 1991; Peulvast and Masson, 1993; Lucchitta et al., 1994; Peulvast et al., 2001).

ANALYSES

Structural Analysis

The amount of lateral shortening on the margins of the Thaumasia Plateau, particularly the Coprates Rise and the Thaumasia Highlands, as well as the finer-scale wrinkle ridges of Solis Planum can be constrained by the equal-area method (Mitra and Namson, 1989). Assuming conservation of cross-sectional area, one can solve for the combinations of depth to the detachment and the displacement needed to raise material in individual wrinkle ridges or in the uplifted frontal anticline defined by the Coprates Rise and the Thaumasia Highlands.

MOLA-derived topographic profiles across the Thaumasia Plateau were used to project the regional far-field slope through the Coprates Rise and the Thaumasia Highlands (Fig. 10). The "excess" cross-sectional area measured from these profiles reveals areas of 340–730 km^2 above the regional topographic trend across these uplands (Mitra and Namson, 1989). A wide range of combinations of depth to detachment and net displacement distance are compatible with the excess cross-sectional area of the Coprates Rise and the Thaumasia Highlands. Judging from the maximum local depth of the extensional features in Noctis Labyrinthus, the basal detachment is >8 km deep. The floor of Hebes Chasma also lies ~8 km below the surrounding plains. Hence, following Mitra and Namson (1989), deformation consistent with an 8- to 10-km-deep basal décollement corresponds to 30–90 km of translation for the deeper structure responsible for the compressional uplands. Across the 3500 km width of shortening, from the frontal escarpment to the wrinkle ridges farthest updip, this entails an overall shortening strain of <3%.

In contrast to these larger compressional features, the 200–300 m height and 10–30 km width of the wrinkle ridges indicate an "excess" cross-sectional area of only ~6–9 km^2. Calculated solutions for these smaller compressional features indicate comparable detachment depths and net displacement of 1–10 km for the wrinkle ridges of Solis Planum. Another way of calculating the maximum depth at which the wrinkle ridges detached is based on their width. Assuming the ridges are pop-ups defined by thrusts, trigonometry indicates a depth to detachment of 1–4 km (Mangold et al., 1998). When combined with this depth range, our measurements of "excess" area yields shortening estimates of 1.5–9 km for individual wrinkle ridges.

Even the greatest displacement and uplift implied by this analysis represents little finite strain. Deformation need not have occurred evenly with depth and is likely to have been concentrated as shear zones in particularly weak layers. Indeed, the deformation represented by the compressional highlands on the southern margin of the Thaumasia Plateau and the wrinkle ridges on the plateau imply décollements at different depths.

Stability Analysis

Despite the striking morphological similarity, a key problem with interpreting the Thaumasia Plateau as a coherent continental-scale landslide is that the general slope across Solis Planum is only ~1° from Syria Planum across the Thaumasia Plateau to the far side of either the Coprates Rise or the Thaumasia Highlands. From the high point on Syria Planum, the slope decreases gradually until the topography rises several km across the Coprates Rise and the Thaumasia Highlands before descending to the plains of Aonia Terra surrounding the Thaumasia Plateau.

Simple slope-stability analysis shows that groundwater pressure far greater than lithostatic (i.e., artesian) would be required to cause gravity failure of basaltic material on the low topographic gradient across the Thaumasia Plateau. Even the simplest model, the infinite-slope stability model (e.g., Selby, 1993) based on the balance of driving to resisting forces for failure of an infinitely wide surface, predicts unreasonably high pore-water pressures to trigger failure of Coulomb materials on such low-gradient slopes. The model is typically expressed as

$$FS = \frac{\tau}{\sigma} = \frac{C + \left(\rho_s \cdot g \cdot z \cdot \cos^2\theta - \mu\right)\tan\phi}{\rho_w \cdot g \cdot z \cdot \sin\theta \cdot \cos\theta}, \qquad (1)$$

where FS is the factor of safety (which equals 1 at failure); τ and σ are, respectively, the shear and normal stresses acting across the failure plane; ρ_s is the density of the slope-forming material; ρ_w is the density of the pore fluid; g is the acceleration due to gravity (3.72 m s^{-2}); C is cohesion; ϕ is the friction angle; z is the depth to the slide plane; θ is the ground slope; and μ is the pore-water pressure in void spaces at the slide plane ($\mu = \rho_w gh$, where h is pore-water pressure head).

Rearranging and solving Equation 1 for FS = 1 provides the critical pore-water pressure, μ_c, for slope failure from

$$\mu_c = \rho_s \cdot g \cdot z \cdot \cos^2\theta - \left(\frac{\rho_w g \cdot z \cdot \sin\theta \cdot \cos\theta - C}{\tan\phi}\right). \qquad (2)$$

Solving for the critical hydraulic head required to trigger slope failure [given by $h_c = \mu_c/(\rho_w g)$] of a 10-km-thick section of crust typical of basaltic lava flows (C = 2 MPa; ϕ = 30°; ρ = 3000 kg m^{-3}) down a 1° regional slope, Equation 2 predicts that almost 22 km of artesian head (i.e., h_c = 31.7 km) would be required. Drag along the lateral boundaries would increase the frictional resistance to gravity spreading even more than this simple analysis indicates. Hence, either the material forming the slope must be failing on highly (and unrealistically) overpressured material, or parts of the plateau-forming material are very weak, or viscous. In contrast to even saturated piles of granular basalt, salt deforms viscously at ambient temperatures on both Earth and Mars, as discussed further below.

SALT TECTONICS

Mechanical Properties of Salts

The observations described above are consistent with continental-scale gravity spreading involving thin-skinned (i.e., ≤10-km-thick) deformation of part or all of the megaregolith, consisting of ancient impact breccia, salts, ice, overlying and/or interbedded ash, volcanic breccia and lava flows. The two distinct styles of deformation in and around the Thaumasia Plateau—large compressional highlands and small wrinkle ridges—indicate a likelihood of décollements at multiple levels, and perhaps several deformation phases. In addition, a regional gravity low that corresponds to the Thaumasia Plateau (Zuber et al., 2000) is consistent with burial of a thick pile of materials having lower than average density (like salts). Finally, the high concentration of rampart craters on Solis Planum would also be consistent with impacts into shallowly buried and potentially hydrous salts. Such craters have halos of granular material that flowed away from the impact and have been interpreted as evidence for near-surface ice (Barlow et al., 2001) or hydrous salts (Komatsu et al., 2007).

Most rocks (other than shales) have relatively similar frictional strengths in the upper crust (Byerlee, 1978), but salts are several orders of magnitude weaker and thus prone to viscous creep (Weijermars et al., 1993). An equally striking difference is that on Earth the brittle-ductile transition for salts can be as shallow as a few meters, as shown by salt glaciers in Iran (Talbot, 1998; Talbot and Aftabi, 2004). Salts deform ductilely as a power-law or Newtonian viscous fluid at temperatures and pressures ambient on Earth. They have virtually no yield strength and flow subaerially at rates that can exceed 1 m yr^{-1} under small gravitational shear stresses provided by topographic slopes of <5° (Talbot et al., 2000; Talbot and Aftabi, 2004). The effective viscosity of rock salt is estimated as ~10^{18} Pa s from rock mechanics (van Keken et al., 1993) and modeling of Interferometric Synthetic Aperture Radar (InSAR)-derived uplift data from the Mount Sedom diapir, Israel (Weinberger et al., 2006). Rock salt's viscosity decreases as grain size decreases and trace water content and temperature increase. Salts are extremely weak and can support little shear traction—an ideal property for a basal detachment for fold-and-thrust belts (Davis and Engelder, 1985; Letouzey et al., 1995; Rowan et al., 2004). Indeed, terrestrial fold and thrust belts over salt detachments can have very low (<1°) topographic dips. Salt-based fold-and-thrust belts typically widen downslope, support regularly spaced folds of weak vergence, and exhibit abrupt changes in deformational style at their margins (Davis and Engelder, 1985)—features that characterize the Thaumasia Plateau. In particular, a complex of thrusts (like those along the Coprates Rise) commonly forms along frontal anticlines (such as the Coprates Rise and the Thaumasia Highlands) at the edge of salt basins where resistance to translation climbs abruptly. In addition, strata above a mobile salt layer often appear to expand radially toward the salt-free foreland (Davis and Engelder, 1985; Gaullier and Vendeville, 2005), resulting in margin-parallel, extensional grabens such as those at Claritas Fossae (Tanaka and Davis, 1988) and the Thaumasia Highlands (Grott et al., 2007).

The relative weakness of evaporites is due to creep-related recrystallization even at low differential stresses and low temperatures (20–200 °C) (Schreiber and Helman, 2005). Halite flows viscously at terrestrial surface temperatures, as shown by salt glaciers. In contrast, anhydrite deforms as a brittle material up to confining pressures of 15 MPa (Liang et al., 2007). Anhydrite begins to recrystallize at ~120 °C and begins to creep at temperatures >150 °C, and even lower temperatures at higher pressures (Müller and Briegel, 1978).

Could deformation of salt or salt-rich deposits on Mars explain the morphology of the Thaumasia Plateau despite the low topographic slope driving the deformation? Temperatures and confining pressures necessary for creep of salts would have existed within the upper 10 km of the martian crust during Hesperian times, assuming martian surface temperature of 218 K, crustal density of 3000 kg/m^3, thermal conductivity of 1.7 W/mK, heat capacity of 840 J/kgK, and heat fluxes of 100 mW/m^2 for Hesperian conditions and 30 mW/ m^2 for present conditions (Stevenson et al., 1983; Clifford and Parker, 2001) (Fig. 11). Moreover, below several km depth the martian crust could have hosted confined aquifers (i.e., reached temperatures >273 K) that,

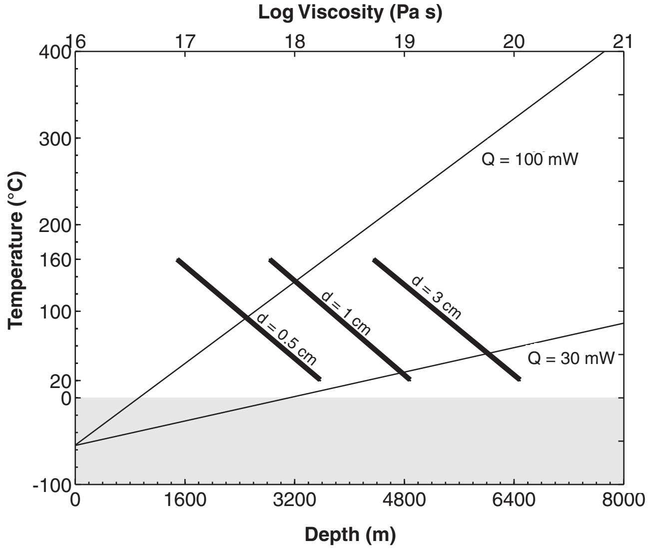

Figure 11. Calculated martian geotherms based on a surface temperature of −55 °C, a heat flux of 100 mW/m^2 (Hesperian, upper curve) or 30 mW/m^2 (present-day, lower curve), a crustal density of 3000 kg/m^3, thermal conductivity of 1.7 W/mK), and a heat capacity of 840 J/kgK. Also shown are effective viscosity-temperature curves for rock salt (halite), indicating decreasing viscosity (more effective detachment) with increasing temperature and decreasing mean grain sized (after van Keken et al., 1993). Gray shading shows temperatures <0 °C.

depending upon the material composition of the crust, could have been quite extensive. Water greatly weakens evaporites, even in mere traces (0.01%) (Urai et al., 1986), and wet gypsum aggregates creep more readily than dry gypsum aggregates (de Meer and Spiers, 1995). Creep rates for wet granular gypsum increase by up to 50 times if the pore fluid is saline, as is typical in mixed evaporites (de Meer and Spiers, 1999). Hence, Tharsis-related heating could destabilize salt deposits, triggering creep and flow down the flank of Syria Planum, even without injection of magma or hot water from below.

Terrestrial Analogs

Gravity-spreading systems detaching on salts and comprising an updip extensional zone linked to a downdip shortening zone are common on Earth, especially on divergent continental margins. Well-known examples include the Gulf of Mexico, the Brazilian and Angolan margins, the Mediterranean Basin, and the North Sea; lesser-known examples are in the Red Sea, Scotian Basin (Canada), and Majunga Basin (Madagascar). The seaward limit of deformation typically coincides either with the limit of autochthonous salts in the original basin, or with the basinward front of advancing allochthonous salt sheets. The estimated strain of <3% across the Thaumasia Plateau is less than the 6% shortening of the Mississippi Fan fold belt, the most intensely studied salt-based fold belt on a passive continental margin (Rowan et al., 2004). Thus, apart from its great size, the requirements for salt-based gravity spreading of the Thaumasia Plateau are modest by the standards of salt tectonics.

From this range of terrestrial examples, we highlight two from the northern Gulf of Mexico as partial analogs for Thaumasia. Whiting Dome (Fig. 12) is one of hundreds of salt diapirs on the lower continental slope. Above a 24-km-long tablet of diapiric allochthonous salt, its Quaternary siliciclastic roof has moved downslope ~1 km by gravity spreading (Peel et al., 1995). A trailing graben at its updip end marks an extensional zone where the roof, detaching on salt, pulled away from the salt-free surrounding area. Conversely, a zone of uplift and probable overthrusting marks shortening at the downdip end of the system. These two zones are linked by a translational zone, whose lateral margins of strike-slip comprise either a principal fault or an en echelon array of transtensional normal faults. Multibeam bathymetry (Divins and Metzger, 2007) shows that apart from the minor trailing graben, the rest of this gravity-spreading system is elevated 200–400 m above the regional datum. The relief is strongly asymmetric, with high elevations concentrated in a frontal bulge caused by inflation of the underlying allochthonous salt. A much larger frontal bulge created by salt tectonics is the >750-km-long Sigsbee Escarpment in the Gulf of Mexico. This escarpment marks the seaward front of the allochthonous salt canopy, created by coalescence of hundreds of salt diapirs, which provides a detachment for gravitational spreading. Hence, the salt-cored Sigsbee Escarpment provides a terrestrial example of a massive frontal anticline and expression of uplift and shortening in the toe of the gravity-spreading system, which resembles the eastern and southern rim of the Thaumasia Plateau.

The Needles area of Canyonlands National Park, Utah, provides a terrestrial analog for the finer-scale extension parallel to the margins of some Valles Marineris chasmata. At The Needles, the Paradox Formation, a cyclic sequence of evaporites, black shale, and carbonates (Hite, 1968), consists of about two-thirds halite and just over 5% anhydrite (Schultz-Ela and Walsh, 2002). These evaporites form a detachment layer along which lateral spreading formed a stepped series of grabens in response to incision of the Colorado River. Erosion through the overlying sedimentary rock into the underlying salts during the past several million years (McGill and Stromquist, 1979) removed the downdip confinement for the salt deposits and lateral support of their overburden, which spread down a 1°–2° décollement toward the canyon, as simulated by finite-element modeling (Schultz-Ela and Walsh, 2002). Equivalent deformation on Mars could involve volcanic ash (cemented to some degree by salts) and lava flows above salts (or ice and salt-cemented deposits). Welded or cemented tuffs and lava flows would act mechanically much like lithified sedimentary rock when subject to viscous flow of an underlying layer.

Terrestrial orogenic belts also exhibit numerous examples of regionally extensive, thin-skinned deformation that serve as potential analogs for the shortening zone of the Thaumasia Plateau. Davis and Engelder (1985) identified 16 examples in which terrestrial fold-and-thrust belts occur at least in part on top of salt beds. In particular, the Appalachian Plateau in western New York and Pennsylvania provides a well-documented example of an extensive, outward-propagating fold-and-thrust belt detached on relatively thin (~75 m thick) salt beds where the limit of substantial folding corresponds to the extent of salt (Rogers, 1963; Davis and Engelder, 1985). At the termination of the salt beds, the largest anticline formed where the accumulated basal slip abruptly converged into splay faults as slip cut upward to the surface (Rogers, 1963; Davis and Engelder, 1985), much like at the base of the Thaumasia Highland and Coprates Rise.

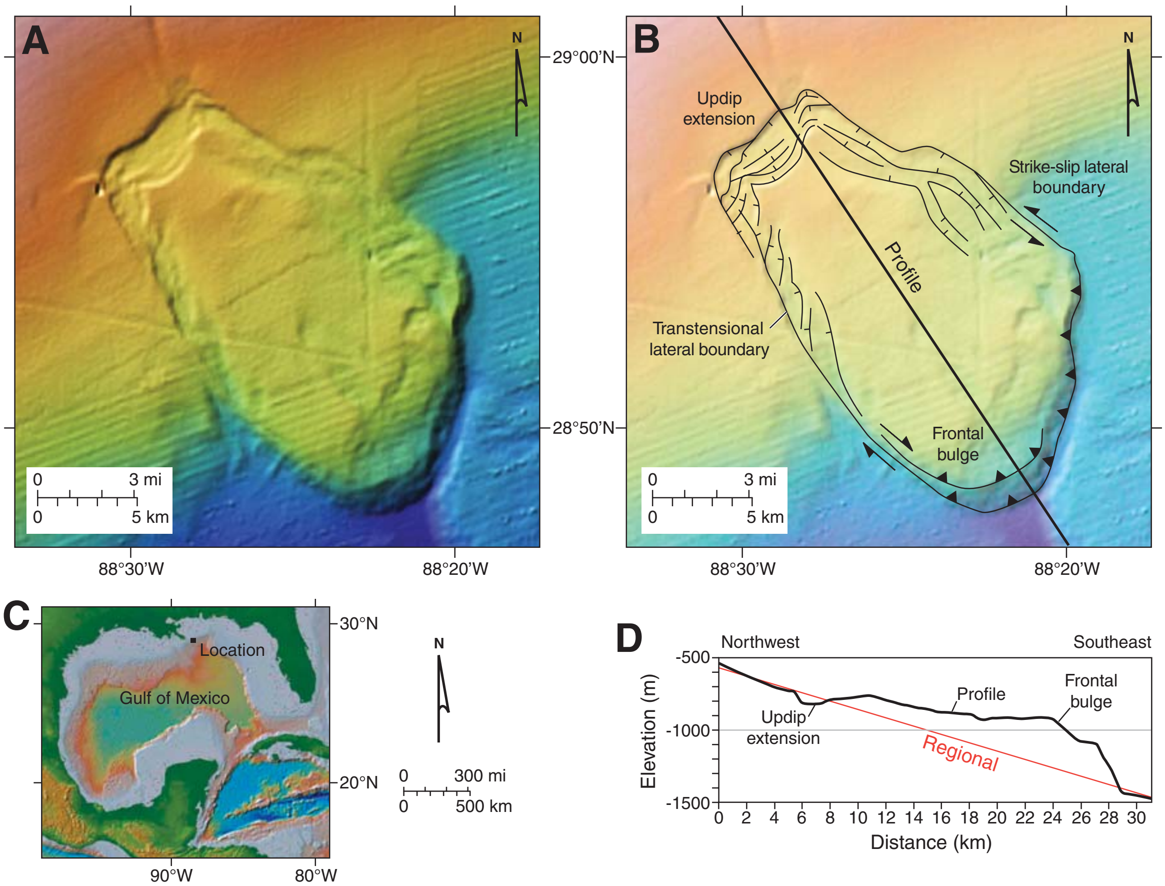

Figure 12. Whiting Dome as a smaller-scale terrestrial analog for gravity spreading detaching on salt. This dome comprises a Quaternary sedimentary veneer detaching on an allochthonous salt sheet. (A) Shaded-relief map having 2× vertical exaggeration, with highs and lows shown as warm and cool colors, respectively. Structural interpretation, based on a deeper map from Peel et al. (1995). (C) Location on the continental slope of the northern Gulf of Mexico. (D) Profile down regional dip; line of section shown in (B). A small part of the diapir crest has sagged below the regional datum because of extension. However, most of the diapir crest has risen asymmetrically several hundred meters above regional because of salt inflation due to downdip salt flow. Bathymetric data in (C) from Smith and Sandwell (1997). All other bathymetric data from Divins and Metzger (2007).

Moreover, the 300-km-long, 70-km-wide, fold-and-thrust belt of the Jura Mountains in central Europe formed above a ~100-m-thick, salt-rich décollement composed of gypsum, anhydrite, and halite, above which Mesozoic sediments are deformed into thrusts and boxfold anticlines, partly thrust-cored, separating broader synclines (Laubscher, 1975, 1992; Bitterli, 1990; Sommaruga, 1999).

In addition, several studies have envisaged anticlines in Washington State's Columbia River basalts as terrestrial analogs for martian wrinkle ridges (e.g., Plescia and Golombek, 1986; Watters, 1988; Watters and Robinson, 1997). In particular, Watters and Robinson (1997) found no evidence that martian wrinkle ridges accommodate vertical offsets between adjacent structural blocks so are unlikely to be the surface expression of deep-penetrating faults. Instead, they favored the anticlinal ridges of the Columbia Plateau in eastern Washington as an analog in which horizontal compression occurs along weak sedimentary interbeds within lava flows. Seismic and gravity data show no evidence of deeply rooted thrust faults beneath the anticlinal ridges of the Columbia Plateau, indicating that the thrust faults responsible for the anticlines occur on weak beds within the deforming sequence of basalt flows (Saltus, 1993; Jarchow et al., 1994), grossly analogous to what we hypothesize for the wrinkle ridges of the Thaumasia Plateau.

HYDROLOGIC POTENTIAL

The base of the upper crust of Mars separates massive rock from a weaker, overlying megaregolith made of layered ash, impact breccia, lava flows, ice, and salts. Although this contact is not clearly exposed, it must involve a major lithologic and strength contrast. Thickness estimates of this megaregolith vary from 1 to 10 km (Clifford, 1993). Consequently, we envision deformation within a regolith consisting of an intermixed—and likely variably stratified and brecciated—pile of lava flows, ash, salts, and ice. Heating from Tharsis and/or crustal thickening could not only trigger flow of buried salts, but could further enhance deformation by dewatering hydrous salts and melting ground ice. Once deformation began along a basal décollement, even modest shear heating (Scholz, 1980) would further dewater evaporites or melt cryospheric ice. Hence, heating of a regolith containing salt beds or salt-ice mixtures would create sulfate-rich brines and soften the salt. At the same time, topographic loading by volcanic effusia from Tharsis and/or Syria Planum would increase the slope, add overburden, and possibly induce hydraulic fracturing. Such fractures could penetrate the cryosphere and provide hydrologic connection from a confined aquifer at the base of the regolith up to the surface.

The calculated martian geotherm discussed above indicates that a liquid-water aquifer would be stable above the inferred 8- to 10-km-deep décollement. Thus, fracturing in the toe of the deforming region would link a confined aquifer to outlets at the surface. Indeed, models of hydrofracturing by overpressured fluids predict growth of integrated fracture networks in a self-organizing process that can rapidly transmit large fluid fluxes (Bons and van Milligen, 2001). Were fractures to penetrate the cryosphere and link a confined aquifer with the martian atmosphere, the connection of a potentially overpressured system with a near vacuum would rapidly expel fluids at the surface. In a different context, Rodríguez et al. (2007) proposed that thrust faulting disrupted precipitation-generated aquifers in southwestern Chryse Planitia, leading to outflows and subsidence in this region.

Curiously, the major outflow channels around Valles Marineris (Echus, Juventae, and Coprates chasmata) are all sourced at similar elevations of ~3.5 km above the martian datum (Fig. 9). This unlikely coincidence could be explained by these outlets representing locations where fractures from within or the sole of the "mega-slide" reached close enough to the surface to focus discharge at the margin of the deforming area. Fractures penetrating through the cryosphere to the surface would allow fluids to vent under elevated hydraulic head within the deforming zone, due in part to the topographic head defined by the 5 km elevation difference within the slide mass from Syria Planum to the outflow sources. Given the substantial topographic head within the aquifer, overpressured fluids reaching the surface could discharge as fountains. If the internal plumbing of the "mega-slide" was the source for the outburst floods, then the headward opening of the main trough of Valles Marineris from Coprates Chasma along a preexisting radial fracture zone would have captured the source area for the Echus and Juventae outflows, routing residual discharge out through Coprates Chasma and shutting off the other surface vents.

How much flow could the aquifer support assuming reasonable hydrologic conductivities and the >5 km of topographic head within the deforming region? Could such an aquifer account for the discharges estimated previously from Echus, Juventae, and Coprates chasmata? Although details of the subsurface materials and plumbing are speculative, we can broadly estimate a reasonable range of potential discharges based on the cross-sectional areas for the outflow sources and estimated values for the permeability and head gradient. The discharge from an aquifer supplying outflow sources can be related to aquifer properties through

$$Q = \left(\frac{k\rho}{\mu}\right)\left(\frac{\mathrm{d}h}{\mathrm{d}x}\right)A, \qquad (3)$$

where Q is the discharge (m^3 s^{-1}); k is the horizontal permeability of the aquifer (m^2); ρ is the density of water (1000 kg m^{-3}); μ is the dynamic viscosity of water (10^{-3} Pa s); dh/dx is the head gradient in the aquifer; and A is the cross-sectional area contributing flow (m^2) (e.g., Carr, 1979; Head et al., 2003; Manga, 2004). Potential cross-sectional areas for the aquifers supplying the outflow channels from Echus, Juventae, and Coprates chasmata range from the roughly 10^3 km^2 cross-sectional area of Juventae Chasma (10 km deep by 100 km across) to the $>10^4$ km^2 cross-sectional area for the walls of Melas and Coprates chasmata (10 km deep by >1000 km long). We assume head gradients from 0.01 to 0.1 and a range of permeabilities from 10^{-9} m^2, as adopted by Manga (2004) for a regional-scale permeability of lava flows, to 10^{-7} m^2, used by Head et al. (2003) to define an upper limit for highly permeable deposits such as breccia or gravel. Incorporating this range of parameter values into Equation 3 predicts discharges of from 10^4 to $>10^8$ m^3 s^{-1}, a range that overlaps with discharge estimates of 10^7 to 10^9 m^3 s^{-1} for martian floods that formed Kasei Valles and Ares Vallis (Robinson and Tanaka, 1990; Carr, 1996; Komatsu and Baker, 1997). Hence, estimated discharges are large enough to potentially supply estimated outflow volumes, although requiring permeabilities and head gradients at the high end of the reasonable range of aquifer properties.

Additional evidence for substantial discharge from a confined aquifer is given by evidence for "hydrothermal" springs along the margin of the Thaumasia Plateau in the Thaumasia Highlands and Coprates Rise (Tanaka et al., 1998). Valleys here have low drainage densities and cluster near evident geologic features, which Tanaka et al. (1998) interpreted to suggest a subsurface origin, such as flow from within a tectonically overpresssured aquifer. Moreover, warm fluid moving up through permafrost would enlarge conduits. Thus initial fracturing, venting, and seepage could lead to the growth of larger conduits through thermal feedback. The fastest growing conduits would eventually capture most of the discharge and potentially drain the aquifer, curtailing discharges from smaller outlets.

Regional groundwater flow down the pre-Tharsis subsurface gradient defined by the base of the mega-regolith would favor discharge outlets on the down-gradient, northeastern side of the aquifer—as observed—and may explain why the NE side of the "mega-slide" produced major outflow channels. Alternatively, two-phase deformation, with a late Noachian event in the south and a later concentration of further deformation to the north could account for aquifer breaching and venting to the north.

SOURCE AND TIMING OF DEFORMATION

The circular shape and elevation of Syria Planum, the highest part of the gravity-spreading system and presumed source of the spreading, are consistent with an underlying igneous plume, which later collapsed after extrusion. Tanaka and Davis (1988) attributed a dense array of annular fractures around the rim of Syria Planum to collapse following magma withdrawal during extrusion of lava flows forming Syria Planum and adjoining regions. Uplift and heating before collapse could have provided the heat and topographic head to initiate deformation.

But what of the nature of the décollement? Structural analyses support the inference of multiple detachments—a deeper surface for deformation of the Coprates Rise and Thaumasia Highlands and shallower detachments for the wrinkle ridges. Either ice or salts could detach and flow along what need not be a single, originally continuous layer. Ice exhibits viscoplastic behavior in which creep becomes increasingly power-law as grain size increases (Duval et al., 1983). Ice-rock mixtures in the martian megaregolith would also be viscoplastic, although with a higher viscosity than clean ice (Durham et al., 1992). As in salts, creep of ice-rich layers can therefore localize strain as ductile shear zones within layered strata. Hence, the basal detachments for gravity spreading could be impure salts or ice, or some combination thereof, as well as the base of the regolith for a deeper detachment.

Deformation of the Thaumasia Plateau involves Noachian to Late Hesperian units, beginning with Syria-centered volcanism and major deformation phases of the Thaumasia Plateau, which overlap in age (Dohm and Tanaka, 1999). Detailed mapping by Dohm and Tanaka (1999) indicates a sharp decline of normal faulting in the early to Late Hesperian, generation of wrinkle ridges in the Late Noachian to Early Hesperian, extension of Noctis Labyrinthus, and opening of the chasmata of Valles Marineris in the Late Hesperian. Thus, the Coprates Rise and Thaumasia Highlands could have deformed first, fol-

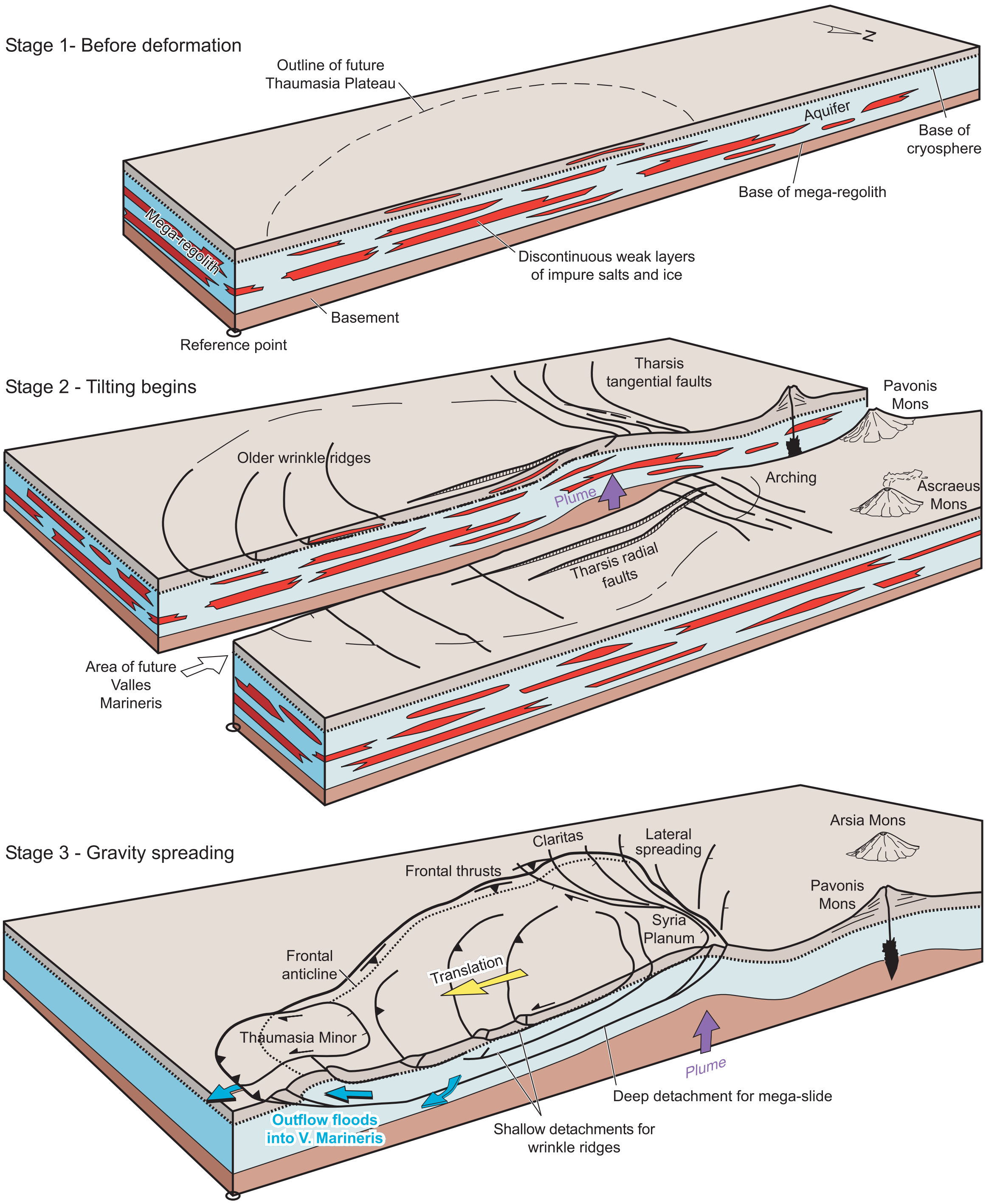

Figure 13. Schematic illustration (not to scale) of the deformation of the Thaumasia Plateau as a "mega-slide" formed by continental-scale salt tectonics. In stage 1, discontinuous layers of salts, ice, and impact breccia accumulate in Noachian time as megaregolith before the growth of Tharsis, perhaps as surface evaporites, or subsurface precipitates during impact-driven generation of the brecciated martian megaregolith. In stage 2, the rise of the Tharsis volcanic province and later arching of Syria Planum above a suspected plume increased both the regional heat flux and local topographic slope, loading the region with ash and lava flows and producing radial extension faults that may have penetrated through the regional cryosphere. In stage 3, layers of salts, ice, and basaltic debris within the regolith provided multiple detachments for the gravity spreading southeastward, possibly in response to further intrusion under Syria Planum. In addition, the aquifer below the cryosphere found outlets to the surface along the chasmata of Valles Marineris where the basal décollement cuts upward to intersect radial extension cracks projecting from Tharsis. This connection rapidly drained the extensive confined aquifer, which had substantial topographic head within the deforming zone. Drainage then carved the outflow channels.

lowed by Thaumasia Minor and Valles Marineris in a second phase of deformation. Far less clear is the time separating these events, especially because of the overlapping spread in potential ages inverted from crater counts (e.g., Dohm and Tanaka, 1999). Nonetheless, deformation soon after volcanic extrusion from Syria Planum could also account for deformation of the older Noachian surface, because crater counts constrain the time of surface formation—not its deformation. Many craters on the Noachian age surfaces are deformed, whereas craters on the Late Hesperian "last flows" from Syria Planum are undeformed. Hence, it is possible that much of the deformation of the Thaumasia Plateau arose from a single extended event or multiple events in Late Hesperian time. In addition, whereas the estimated Noachian heat flow would produce substantial salt softening and a thick crustal aquifer below a several-km-thick cryosphere, the reduced modern heat flow would result in a thin deeper crustal aquifer below a thicker cryosphere and therefore substantially less potential for mobility under present conditions.

SUMMARY AND CONCLUSIONS

Analysis of structural and geomorphologic data indicates that deformation of the Thaumasia Plateau is consistent with a "mega-slide" driven by continental-scale salt tectonics. Our proposed hypothesis involves several episodes (Fig. 13).

First, exposures in the walls of the Valles Marineris chasmata suggest that extensive "salt" deposits or cements accumulated before the growth of Tharsis, perhaps in Early Noachian ephemeral lakes or shallow-water bodies in a paleobasin like that envisioned by Dohm et al. (2001). Alternatively, salt-rich bodies may have been formed through regional groundwater flow within porous aquifers (Andrews-Hanna et al., 2007), or intermittent precipitation during impact-driven generation of the brecciated martian megaregolith (Segura et al., 2002). Dry atmospheric deposition of extensive salt-rich deposits is also possible (Catling et al., 2006).

Second, the rise of Tharsis and subsequently Syria Planum increased both the regional heat flux and local topographic slope, loading the region with ash and lava flows and producing radial extension cracks that may have penetrated through the regional cryosphere. Such heating would have melted ground ice and dewatered hydrous salts, and potentially increased subsurface hydrologic connectivity, and topographic loading would have contributed to producing overpressured fluids.

Third, layers of salts, ice, and basaltic debris within the regolith provided multiple detachments for the gravity spreading southeastward, possibly in response to initial development of Tharsis and subsequent intrusion under Syria Planum.

Finally, fractures from the basal décollement cut through an aquifer at the base of the cryosphere (Carr, 1979). Where these deep fractures intersected radial extension cracks projecting from Tharsis, the aquifer found ready outlets to the surface along Valles Marineris and environs. These connections rapidly drained at least a portion of the extensive confined aquifer, which had substantial topographic head within the deforming zone. The resulting drainage carved the outflow channels.

This single hypothesis provides a unifying explanation for: (1) forming thrust faults and the massive frontal anticline along the Coprates Rise and Thaumasia Highlands; (2) strike-slip and extension on the western edge of Solis Planum; (3) the location, linearity, and depth of the Valles Marineris chasmata; (4) the regional concentration of rampart craters on the Thaumasia Plateau; and (5) the similar elevations for the origin of the Echus, Juventae, and Coprates outflow channels.

ACKNOWLEDGMENTS

We thank Darrel Cowan for discussions of balanced cross sections and Harvey Greenberg and Charles Kiblinger for help in preparing the figures. M. Jackson was supported by the Applied Geodynamics Laboratory consortium. This paper is published with permission of the Director, Bureau of Economic Geology. A. Gillepsie's participation was partly supported by National Aeronautics and Space Administration's Mars Data Analysis Program, contract NNX07AV77G.

REFERENCES CITED

Anderson, R.C., Dohm, J.M., Golombek, M.P., Haldemann, A.F.C., Franklin, B.J., Tanaka, K.L., Lias, J., and Peer, B., 2001, Primary centers and secondary concentrations of tectonic activity through time in the western hemisphere of Mars: Journal of Geophysical Research, v. 106, p. 20,563–20,585, doi: 10.1029/2000JE001278.

Anderson, S., and Grimm, R.E., 1998, Rift processes at the Valles Marineris, Mars: Constraints from gravity on necking and rate-dependent strength evolution: Journal of Geophysical Research, v. 103, p. 11,113–11,124.

Andrews-Hanna, J.C., Phillips, R.J., and Zuber, M.T., 2007, Meridiani Planum and the global hydrology of Mars: Nature, v. 446, p. 163–166, doi: 10.1038/nature05594.

Anguita, F., Farelo, A.-F., López, V., Mas, C., Muñoz-Espadas, M.-J., Márquez, A., and Ruiz, J., 2001, Tharsis dome, Mars: New evidence for Noachian-Hesperian thick-skin and Amazonian thin-skin tectonics: Journal of Geophysical Research, v. 106, p. 7577–7589.

Anguita, F., Fernández, C., Cordero, G., Carrasquilla, S., Anguita, J., Núñez, A., Rodríguez, S., and García, J., 2006, Evidences for a Noachian-Hesperian orogeny in Mars: Icarus, v. 185, p. 331–357, doi: 10.1016/j.icarus.2006.07.026.

Baker, V.R., and Milton, D.J., 1974, Erosion by catastrophic floods on Mars and Earth: Icarus, v. 23, p. 27–41, doi: 10.1016/0019-1035(74)90101-8.

Banerdt, W.B., Phillips, R.J., Sleep, N.H., and Saunders, R.S., 1982, Thick shell tectonics on one-plate planets: Applications to Mars: Journal of Geophysical Research, v. 87, p. 9723–9733.

Barlow, N.G., Koroshetz, J., and Dohm, J.M., 2001, Variations in the onset diameter for Martian layered ejecta morphologies and their implications for subsurface volatile reservoirs: Geophysical Research Letters, v. 28, p. 3095–3098.

Bibring, J.-P., et al., 2006, Global mineralogical and aqueous history derived from OMEGA/Mars Express data: Science, v. 312, p. 400–404, doi: 10.1126/science.1122659.

Bigot-Cormier, F., and Montgomery, D.R., 2007, Valles Marineris landslides: Strength limit to Martian relief?: Earth and Planetary Science Letters, v. 260, p. 179–186, doi: 10.1016/j.epsl.2007.05.028.

Bitterli, T., 1990, The kinematic evolution of a classical Jura fold: A reinterpretation based on 3-dimensional balancing techniques (Weissenstein anticline, Jura Mountains, Switzerland): Eclogae Geologicae Helvetiae, v. 83, p. 493–511.

Blasius, K.R., Cutts, J.A., Guest, J.E., and Masursky, H., 1977, Geology of the Valles Marineris: First analysis of imaging from the Viking 1 Orbiter primary mission: Journal of Geophysical Research, v. 82, p. 4067–4091.

Bons, P.D., and van Milligen, B.P., 2001, New experiment to model self-organized critical transport and accumulation of melt and hydrocarbons from their source rocks: Geology, v. 29, p. 919–922, doi: 10.1130/0091-7613(2001)029<0919:NETMSO>2.0.CO;2.

Borraccini, F., Di Achille, G., Ori, G.G., and Wezel, F.C., 2007, Tectonic evolution of the eastern margin of the Thaumasia Plateau (Mars) as inferred from detailed structural mapping and analysis: Journal of Geophysical Research, v. 112, p. E05005, doi: 10.1029/2006JE002866.

Byerlee, J.D., 1978, Friction of rocks: Pure and Applied Geophysics, v. 116, p. 615–626, doi: 10.1007/BF00876528.

Carr, M.H., 1979, Formation of Martian flood features by release of water from confined aquifers: Journal of Geophysical Research, v. 82, p. 2995–3007.

Carr, M.H., 1996, Water on Mars: New York and Oxford, Oxford University Press.

Catling, D.C., Wood, S.E., Leovy, C., Montgomery, D.R., Greenberg, H.M., Glein, C.R., and Moore, J.M., 2006, Light-toned layered deposits in Juventae Chasma, Mars: Icarus, v. 181, p. 26–51, doi: 10.1016/j.icarus.2005.10.020.

Chapman, M.G., and Tanaka, K.L., 2001, The interior deposits on Mars: Sub-ice volcanoes?: Journal of Geophysical Research, v. 106, p. 10,087–10,100, doi: 10.1029/2000JE001303.

Christensen, P.R., Jakosky, B.M., Kieffer, H.H., Malin, M.C., McSween, H.Y., Jr., Nealson, K., Mehall, G.L., Silverman, S.H., Ferry, S., Caplinger, M., and Ravine, M., 2004, The Thermal Emission Imaging System (THEMIS) for the Mars 2001 Odyssey Mission: Space Science Reviews, v. 110, p. 85–130, doi: 10.1023/B:SPAC.0000021008.16305.94.

Clifford, S.M., 1993, A model for the hydrologic and climatic behaviour of water on Mars: Journal of Geophysical Research, v. 98, p. 10,973–11,016, doi: 10.1029/93JE00225.

Clifford, S.M., and Parker, T.J., 2001, The evolution of the martian hydrosphere: Implications for the fate of a primordial ocean and the current state of the Northern Plains: Icarus, v. 154, p. 40–79, doi: 10.1006/icar.2001.6671.

Cutts, J.A., and Blasius, K.R., 1981, Origin of martian outflow channels: The eolian hypothesis: Journal of Geophysical Research, v. 86, p. 5075–5102.

Davis, D.M., and Engelder, T., 1985, The role of salt in fold-and-thrust belts: Tectonophysics, v. 119, p. 67–88, doi: 10.1016/0040-1951(85)90033-2.

de Meer, S., and Spiers, C.J., 1995, Creep of wet gypsum aggregates under hydrostatic loading conditions: Tectonophysics, v. 245, p. 171–183, doi: 10.1016/0040-1951(94)00233-Y.

de Meer, S., and Spiers, C.J., 1999, Influence of pore-fluid salinity on pressure solution creep in gypsum: Tectonophysics, v. 308, p. 311–330, doi: 10.1016/S0040-1951(99)00110-9.

Divins, D.L., and Metzger, D., 2007, NGDC Coastal relief model, http://www.ngdc.noaa.gov/mgg/coastal/coastal.html.

Dohm, J.M., and Tanaka, K.L., 1999, Geology of the Thaumasia region, Mars: Plateau development, valley origins, and magmatic evolution: Planetary and Space Science, v. 47, p. 411–431, doi: 10.1016/S0032-0633(98)00141-X.

Dohm, J.M., Ferris, J.C., Baker, V.R., Anderson, R.C., Hare, T.M., Strom, R.G., Barlow, N.G., Tanaka, K.L., Klemaszewski, J.E., and Scott, D.H., 2001, Ancient drainage basin of the Tharsis region, Mars: Potential source for outflow channel systems and putative oceans or paleolakes: Journal of Geophysical Research, v. 106, p. 32,943–32,958, doi: 10.1029/2000JE001468.

Dromart, G., Quantin, C., and Broucke, O., 2007, Stratigraphic architectures spotted in southern Melas Chasma, Valles Marineris, Mars: Geology, v. 35, p. 363–366, doi: 10.1130/G23350A.1.

Durham, W.B., Kirby, S.H., and Stern, L.A., 1992, Effects of dispersate particulates on the rheology of water ice at planetary conditions: Journal of Geophysical Research, v. 97, p. 20,883–20,897.

Duval, P., Ashby, M.F., and Anderman, I., 1983, Rate-controlling processes in the creep of polycrystalline ice: Journal of Physical Chemistry, v. 87, p. 4066–4074.

Frey, H., 1979, Thaumasia: A fossilized early forming Tharsis uplift, Journal of Geophysical Research, v. 84, p. 1009–1023.

Gaullier, V., and Vendeville, B.C., 2005, Salt tectonics driven by sediment progradation: Part II—Radial spreading of sedimentary lobes prograding above salt: American Association of Petroleum Geologists Bulletin, v. 89, p. 1081–1089.

Gendrin, A., Mangold, N., Bibring, J.-P., Langevin, Y., Gondet, B., Poulet, F., Bonello, G., Quantin, C., Mustard, J., Arvidson, R., LeMouélic, S., and the OMEGA team, 2005, Sulfates in Martian layered terrains: The OMEGA/Mars Express view: Science, v. 307, no. 5715, p. 1587–1591, doi: 10.1126/science.1109087.

Golombek, M.P., Anderson, F.S., and Zuber, M.T., 2001, Martian wrinkle ridge topography: Evidence for subsurface faults from MOLA: Journal of Geophysical Research, v. 106, p. 23,811–23,821, doi: 10.1029/2000JE001308.

Grott, M., Hauber, E., Werner, S.C., Kronberg, P., and Newkum, G., 2005, High heat flux on ancient Mars: Evidence from rift flank uplift at Coracis Fossae: Geophysical Research Letters, v. 32, L21201, doi:10/1029/2005GL023894.

Grott, M., Kronberg, P., Hauber, E., and Cailleau, B., 2007, Formation of the double rift system in the Thaumasia Highlands, Mars: Journal of Geophysical Research, v. 112, p. E06006, doi: 10.1029/2006JE002800.

Head, J.W., Wilson, L., and Mitchell, K.L., 2003, Generation of recent massive water floods at Cerberus Fossae, Mars by dike emplacement, cryospheric cracking, and confined aquifer groundwater release: Geophysical Research Letters, v. 30, no. 11, p. 1577, doi: 10.1029/2003GL017135.

Hite, R.J., 1968, Salt deposits of the Paradox Basin, southeast Utah and southwest Colorado: Boulder, Colorado, Geological Society of America Special Paper 88, p. 319–330.

Hoffman, N., 2000, White Mars: A new model for Mars' surface and atmosphere based on CO_2: Icarus, v. 146, p. 326–342, doi: 10.1006/icar.2000.6398.

Hovland, M., Rueslåtten, H.G., Johnsen, H.K., Kvamme, B., and Kuznetsova, T., 2006, Salt formation associated with sub-surface boiling and supercritical water: Marine and Petroleum Geology, v. 23, p. 855–869, doi: 10.1016/j.marpetgeo.2006.07.002.

Jarchow, C.M., Catchings, R.D., and Lutter, W.J., 1994, Large-explosion source, wide-recording aperture, seismic profiling on the Columbia Plateau, Washington: Geophysics, v. 59, p. 259–271, doi: 10.1190/1.1443588.

Kargel, J.S., Furfaro, R., Prieto-Ballesteros, O., Rodriguez, J.A.P., Montgomery, D.R., Gillespie, A.R., Marion, G., and Wood, S.E., 2007, Martian hydrogeology sustained by thermally insulating gas and salt hydrates: Geology, v. 35, p. 975–978, doi: 10.1130/G23783A.1.

Komatsu, G., and Baker, V.R., 1997, Paleohydrology and flood geomorphology of Ares Vallis: Journal of Geophysical Research, v. 102, p. 4151–4160, doi: 10.1029/96JE02564.

Komatsu, G., Geissler, P.E., Strom, R.G., and Singer, R.B., 1993, Stratigraphy and erosional landforms of layered deposits in Valles Marineris, Mars: Journal of Geophysical Research, v. 98, p. 11,105–11,121, doi: 10.1029/93JE00537.

Komatsu, G., Ori, G.G., Di Lorenzeo, S., Rossi, A.P., and Neukum, G., 2007, Combinations of processes responsible for Martian impact crater "layered ejecta structures" emplacement: Journal of Geophysical Research, v. 112, p. E06005, doi: 10.1029/2006JE002787.

Lambert, R.St.J., and Chamberlain, V.E., 1978, CO_2 permafrost and martian topography: Icarus, v. 34, p. 568–580, doi: 10.1016/0019-1035(78)90046-5.

Langevin, Y., Poulet, F., Bibring, J.-P., and Gondet, B., 2005, Sulfates in the north polar region of Mars detected by OMEGA/Mars Express: Science, v. 307, p. 1584–1586, doi: 10.1126/science.1109091.

Laubscher, H., 1992, Jura kinematics and the Molasse Basin: Eclogae Geologicae Helvetiae, v. 85, p. 653–675.

Laubscher, H.P., 1975, Viscous components in Jura folding: Tectonophysics, v. 27, p. 239–254, doi: 10.1016/0040-1951(75)90019-0.

Letouzey, J., Colletta, B., Vially, R., and Chermette, J.C., 1995. Evolution of salt-related structures in compressional settings, *in* Jackson, M.P.A., Roberts, D.G., and Snelson, S., eds., Salt tectonics: A global perspective: American Association of Petroleum Geologists Memoir 65, p. 41–60.

Leverington, D.W., 2004, Volcanic rilles, streamlined islands, and the origin of outflow channels on Mars: Journal of Geophysical Research, v. 109, p. E10011, doi: 10.1029/2004JE002311

Liang, W., Yang, C., Zhao, Y., Dusseault, M.B., and Liu, J., 2007, Experimental investigation of mechanical properties of bedded salt rock: International Journal of Rock Mechanics and Mining Sciences, v. 44, p. 400–411, doi: 10.1016/j.ijrmms.2006.09.007.

Lucchitta, B.K., Anderson, D.M., and Shoji, H., 1981, Did ice streams carve martian outflow channels?: Nature, v. 290, p. 759–763, doi: 10.1038/290759a0.

Lucchitta, B.K., Clow, G.D., Geissler, P.E., McEwen, A.S., Schultz, R.A., Singer, R.B., and Squyres, S.W., 1992, The canyon system on Mars, *in* Kieffer, H.H., et al., eds., Mars: Tucson, University of Arizona Press, p. 453–492.

Lucchitta, B.K., Isbell, N.K., and Howington-Kraus, A., 1994, Topography of Valles Marineris: Implications for erosional and structural history: Journal of Geophysical Research, v. 99, p. 3783–3798.

Malin, M.C., and Edgett, K.S., 2000, Sedimentary rocks of early Mars: Science, v. 290, p. 1927–1937, doi: 10.1126/science.290.5498.1927.

Malin, M.C., Danielson, G.E., Ravine, M.A., and Soulanille, T.A., 1991, Design and development of the Mars Orbiter Camera: International Journal of Imaging System Technology, v. 3, p. 76–91.

Manga, M., 2004, Martian floods at Cerberus Fossae can be produced by groundwater discharge: Geophysical Research Letters, v. 31, p. L02702, doi: 10.1029/2003GL018958.

Mangold, N., Allemand, P., and Thomas, P.G., 1998, Wrinkle ridges of Mars: Structural analysis and evidence for shallow deformation controlled by ice-rich décollements: Planetary and Space Science, v. 46, p. 345–356, doi: 10.1016/S0032-0633(97)00195-5.

Masson, P., 1977, Structure pattern analysis of the Noctis Labyrinthus-Valles Marineris regions of Mars: Icarus, v. 30, p. 49–62, doi: 10.1016/0019-1035(77)90120-8.

Masson, P., 1980, Contribution to the structural interpretation of the Valles Marineris-Noctis Labyrinthus-Claritas Fossae regions of Mars: The moon and the planets, v. 22, p. 211–219, doi: 10.1007/BF00898432.

Masson, P., 1985, Origin and evolution of the Valles Marineris region of Mars: Advances in Space Research, v. 5, no. 8, p. 83–92, doi: 10.1016/0273-1177(85)90244-3.

McEwen, A.S., Malin, M.C., Carr, M.H., and Hartmann, W.K., 1999, Voluminous volcanism on early Mars revealed in Valles Marineris: Nature, v. 397, p. 584–586, doi: 10.1038/17539.

McGill, G.E., and Stromquist, A.W., 1979, The grabens of Canyonlands National Park, Utah—Geometry, mechanics, and kinematics: Journal of Geophysical Research, v. 84, p. 4547–4563.

McKenzie, D., and Nimmo, F., 1999, The generation of Martian floods by the melting of ground ice above dykes: Nature, v. 397, p. 231–233, doi: 10.1038/16649.

Mége, D., and Masson, P., 1996a, Stress models for Tharsis formation, Mars: Planetary and Space Science, v. 44, p. 1471–1497.

Mége, D., and Masson, P., 1996b, Amounts of crustal stretching in Valles Marineris, Mars: Planetary and Space Science, v. 46, p. 345–356.

Mellon, M.T., Jakosky, B.M., and Postawko, S.E., 1997, The persistence of equatorial ground ice on Mars: Journal of Geophysical Research, v. 102, p. 19,357–19,369, doi: 10.1029/97JE01346.

Milton, D.J., 1974, Carbon dioxide hydrate and floods on Mars: Science, v. 183, p. 654–656, doi: 10.1126/science.183.4125.654.

Mitra, S., and Namson, J., 1989, Equal-area balancing: American Journal of Science, v. 289, p. 563–599.

Montesi, L.G.J., and Zuber, M.T., 2003, Clues to the lithospheric structure of Mars from wrinkle ridge sets and localization instability: Journal of Geophysical Research, v. 108, p. 1–25.

Montgomery, D.R., and Gillespie, A., 2005, Formation of Martian outflow channels by catastrophic dewatering of evaporite deposits: Geology, v. 33, p. 625–628, doi: 10.1130/G21270.1.

Mueller, K., and Golombek, M., 2004, Compressional structures on Mars: Annual Review of Earth and Planetary Sciences, v. 32, p. 435–464, doi: 10.1146/annurev.earth.32.101802.120553.

Müller, W.H., and Briegel, U., 1978, The rheological behaviour of polycrystalline anhydrite: Eclogae Geologicae Helvetiae, v. 71, p. 397–407.

Nedell, S.S., Squyres, S.W., and Anderson, D.W., 1987, Origin and evolution of the layered deposits in the Valles Marineris, Mars: Icarus, v. 70, p. 409–441, doi: 10.1016/0019-1035(87)90086-8.

Okubo, C.H., and Schultz, R.A., 2004, Mechanical stratigraphy in the western equatorial region of Mars based on thrust fault-related fold topography and implications for near-surface volatile reservoirs: Geological Society of America Bulletin, v. 116, p. 594–605, doi: 10.1130/B25361.1.

Osterloo, M.M., Hamilton, V.E., Bandfield, J.L., Glotch, T.D., Baldridge, A.M., Christensen, P.R., Tornabene, L.L., and Anderson, F.S., 2008, Chloride-bearing materials in the southern highlands of Mars: Science, v. 319, p. 1651–1654.

Peel, F.J., Travis, C.J., and Hossack, J.R., 1995, Genetic structural provinces and salt tectonics of the Cenozoic offshore U.S. Gulf of Mexico: A preliminary analysis, *in* Jackson, M.P.A., Roberts, D.G., and Snelson, S., eds., Salt tectonics: A global perspective: American Association of Petroleum Geologists Memoir 65, p. 153–175.

Peulvast, J.P., and Masson, P.L., 1993, Erosion and tectonics in central Valles Marineris (Mars): A new morpho-structural model: Earth, Moon, and Planets, v. 61, p. 191–217, doi: 10.1007/BF00572245.

Peulvast, J.-P., Mége, D., Chiciak, J., Costard, F., and Masson, P.L., 2001, Morphology, evolution and tectonics of Valles Marineris wallslopes (Mars): Geomorphology, v. 37, p. 329–352, doi: 10.1016/S0169-555X(00)00085-4.

Plescia, J.B., and Golombek, M.P., 1986, Origin of planetary wrinkle ridges based on the study of terrestrial analogs: Geological Society of America Bulletin, v. 97, p. 1289–1299.

Plescia, J.B., and Saunders, R.S., 1982, Tectonic history of the Tharsis Region, Mars: Journal of Geophysical Research, v. 87, p. 9775–9791.

Quantin, C., Allemand, P., Mangold, N., Dromart, G., and Delacourt, C., 2005, Fluvial and lacustrine activity on layered deposits in Melas Chasma, Valles Marineris, Mars: Journal of Geophysical Research, v. 110, E12S19, doi: 10.1029/2005JE002440.

Robinson, M.S., and Tanaka, K.L., 1990, Magnitude of a catastrophic flood event at Kasei Valles, Mars: Geology, v. 18, p. 902–905, doi: 10.1130/0091-7613(1990)018<0902:MOACFE>2.3.CO;2.

Rodríguez, J.A.P., Kargel, J., Crown, D.A., Bleamaster, L.F., III, Tanaka, K.L., Baker, V., Miyamoto, H., Dohm, J.M., Sasaki, S., and Komatsu, G., 2006, Headward growth of chasmata by volatile outbursts, collapse, and drainage: Evidence from Ganges chaos, Mars: Geophysical Research Letters, v. 33, p. L18203, doi: 10.1029/2006GL026275.

Rodríguez, J.A.P., Tanaka, K.L., Kargel, J., Dohm, J.M., Kuzmin, R., Fairén, A.G., Sasaki, S., Komatsu, G., Schulze-Makach, D., and Jianguo, Y., 2007, Formation and disruption of aquifers in southwestern Chryse Planitia, Mars: Icarus, v. 191, p. 545–567, doi: 10.1016/j.icarus.2007.05.021.

Rogers, J., 1963, Mechanics of Appalachian foreland folding in Pennsylvania and West Virginia: American Association of Petroleum Geologists Bulletin, v. 47, p. 1527–1536.

Rowan, M.G., Peel, F.J., and Vendeville, B.C., 2004, Gravity-driven fold belts on passive margins, *in* McClay, K.R., ed., Thrust tectonics and hydrocarbon systems: American Association of Petroleum Geologists Memoir, 82, p. 157–182.

Saltus, R.W., 1993, Upper crustal structure beneath the Columbia River Basalt Group, Washington: Gravity interpretation controlled by borehole and seismic studies: Geological Society of America Bulletin, v. 105, p. 1247–1259.

Schoenfield, E., 1979, Origin of Valles Marineris: Proceedings of the 10th Lunar and Planetary Science Conference, p. 3031–3038.

Scholz, C.H., 1980, Shear heating and the state of stress on faults: Journal of Geophysical Research, v. 85, p. 6174–6184.

Schreiber, B.C., and Helman, M.L., 2005, Criteria for distinguishing primary evaporite features from deformation features in sulfate evaporates: Journal of Sedimentary Research, v. 75, p. 525–533, doi: 10.2110/jsr.2005.043.

Schultz, R.A., 1989, Strike-slip faulting of ridged plains near Valles Marineris, Mars: Nature, v. 341, p. 424–426, doi: 10.1038/341424a0.

Schultz, R.A., 1991, Structural development of Coprates Chasma and western Ophir Planum, central Valles Marineris rift, Mars: Journal of Geophysical Research, v. 96, p. 22,777–22,792, doi: 10.1029/91JE02556.

Schultz, R.A., 1995, Gradients in extension and strain at Valles Marineris, Mars: Planetary and Space Science, v. 43, p. 1561–1566.

Schultz, R.A., 1998, Multiple-process origin of Valles Marineris basins and troughs, Mars: Planetary and Space Science, v. 46, p. 827–834, doi: 10.1016/S0032-0633(98)00030-0.

Schultz, R.A., and Lin, J., 2001, Three-dimensional normal faulting models of the Valles Marineris, Mars, and geodynamic implications: Journal of Geophysical Research, v. 106, p. 16,549–16,566, doi: 10.1029/2001JB000378.

Schultz, R.A., and Tanaka, K.L., 1994, Lithospheric-scale buckling and thrust structures on Mars: The Coprates rise and south Tharsis ridge belt: Journal of Geophysical Research, v. 99, p. 8371–8385.

Schultz-Ela, D.D., and Walsh, P., 2002, Modeling of grabens extending above evaporites in Canyonlands National Park, Utah: Journal of Structural Geology, v. 24, p. 247–275, doi: 10.1016/S0191-8141(01)00066-9.

Segura, T.L., Toon, O.B., Colaprete, A., and Zahnle, K., 2002, Environmental effects of large impacts on Mars: Science, v. 298, p. 1977–1980, doi: 10.1126/science.1073586.

Selby, M.J., 1993, Hillslope materials and processes: Oxford, University Press, 451 p.

Sharp, R.P., 1973, Mars: fretted and chaotic terrain: Journal of Geophysical Research, v. 78, p. 4073–4083.

Smith, W.H.F., and Sandwell, D.T., 1997, Global seafloor topography from satellite altimetry and ship depth soundings: Science, v. 277, p. 1957–1962.

Sommaruga, A., 1999, Décollement tectonics in the Jura foreland fold-and-thrust belt: Marine and Petroleum Geology, v. 16, p. 111–134, doi: 10.1016/S0264-8172(98)00068-3.

Spencer, J.R., and Fanale, F.P., 1990, New models for the origin of Valles Marineris closed depressions: Journal of Geophysical Research, v. 95, p. 14,301–14,313, doi: 10.1029/JB095iB09p14301.

Squyres, S.W., Grotzinger, J.P., Arvidson, R.E., Bell, J.F., III, Calvin, W., Christensen, P.R., Clark, B.C., Crisp, J.A., Farrand, W.H., Herkenhoff, K.E., Johnson, J.R., Klingelhöfer, G., Knoll, A.H., McLennan, S.M., McSween, H.Y., Jr., Morris, R.V., Rice, J.W., Jr., Rieder, R., and Soderblom, L.A., 2004, In situ evidence for an ancient aqueous environment at Meridiani Planum, Mars: Science, v. 306, p. 1709–1714, doi: 10.1126/science.1104559.

Stevenson, D.J., Spohn, T., and Schubert, G., 1983, Magnetism and thermal evolution of the terrestrial planets: Icarus, v. 54, p. 466–489, doi: 10.1016/0019-1035(83)90241-5.

Talbot, C.J., 1998, Extrusions of Hormuz salt in Iran, *in* Blundell, D.J., and Scott, A.C., eds., Lyell: The past is the key to the present: The Geological Society of London, Special Publications, v. 143, p. 315–334.

Talbot, C.J., and Aftabi, P., 2004, Geology and models of salt extrusion at Qum Kuh, central Iran: The Geological Society of London, v. 161, p. 321–334, doi: 10.1144/0016-764903-102.

Talbot, C.J., Medvedev, S., Alavi, M., Shahrivar, H., and Heidari, E., 2000, Salt extrusion at Kuh-e-Jahani, Iran, from June 1994 to November 1997, *in* Vendeville, B., Mart, Y., and Vigneresse, J-L., eds., Salt, shale and igneous diapirs in and around Europe: The Geological Society of London, Special Publications, v. 174, p. 93–110.

Tanaka, K.L., 1999, Debris-flow origin for the Simud/Tiu deposit on Mars: Journal of Geophysical Research, v. 104, p. 8637–8652, doi: 10.1029/98JE02552.

Tanaka, K.L., and Davis, P.A., 1988, Tectonic history of the Syria Planum province of Mars: Journal of Geophysical Research, v. 93, p. 14,893–14,917, doi: 10.1029/JB093iB12p14893.

Tanaka, K.L., and Golombek, M.P., 1989, Martian tension fractures and the formation of grabens and collapse features at Valles Marineris: Proceedings of the Lunar and Planetary Science Conference, v. 19, p. 383–396.

Tanaka, K.L., Golombek, M.P., and Banerdt, W.B., 1991, Reconciling stress and structural histories of the Tharsis region of Mars: Journal of Geophysical Research, v. 96, p. 15,617–15,633, doi: 10.1029/91JE01194.

Tanaka, K.L., Dohm, J.M., Lias, J.H., and Hare, T.M., 1998, Erosional valleys in the Thaumasia region of Mars: Hydrothermal and seismic origins: Journal of Geophysical Research, v. 103, p. 31,407–31,419, doi: 10.1029/98JE01599.

Urai, J.L., Spiers, C.J., Zwart, H.J., and Lister, G.S., 1986, Weakening of rock salt by water during long-term creep: Nature, v. 324, p. 554–557, doi: 10.1038/324554a0.

van Keken, P.E., Spiers, C.J., van den Berg, A.P., and Muyzert, E.L., 1993, The effective viscosity of rocksalt: Implementation of steady-state creep laws in numerical models of salt diapirism: Tectonophysics, v. 225, p. 457–476, doi: 10.1016/0040-1951(93)90310-G.

Vendeville, B.C., 2005, Salt tectonics driven by sediment progradation: Part I, Mechanics and kinematics: American Association of Petroleum Geologists Bulletin, v. 89, p. 1071–1079.

Watters, T.R., 1988, Wrinkle ridges assemblages on the terrestrial planets: Journal of Geophysical Research, v. 93, p. 10,236–10,254, doi: 10.1029/JB093iB09p10236.

Watters, T.R., and Robinson, M.S., 1997, Radar and photoclinometric studies of wrinkle ridges on Mars: Journal of Geophysical Research, v. 102, p. 10,889–10,903, doi: 10.1029/97JE00411.

Weijermars, R., Jackson, M.P.A., and Venderville, B.C., 1993, Rheological and tectonic modeling of salt provinces: Tectonophysics, v. 217, p. 143–174, doi: 10.1016/0040-1951(93)90208-2.

Weinberger, R., Lyakhovsky, V., Baer, G., and Begin, Z.B., 2006, Mechanical modeling and InSAR measurements of Mount Sedom uplift, Dead Sea basin: Implications for effective viscosity of rock salt: Geochemistry Geophysics Geosystems, v. 7, p. Q05014, doi: 10.1029/2005GC001185.

Williams, J.-P., Paige, D.A., and Manning, C.E., 2003, Layering in the wall rock of Valles Marineris: Intrusive and extrusive magmatism: Geophysical Research Letters, v. 30, no. 12, p. 1623, doi: 10.1029/2003GL017662.

Zuber, M.T., and Aist, L.L., 1990, The shallow structure of the martian lithosphere in the vicinity of the ridged plains: Journal of Geophysical Research, v. 95, p. 14,215–14,230, doi: 10.1029/JB095iB09p14215.

Zuber, M.T., et al., 1992, The Mars Observer laser altimeter investigation: Journal of Geophysical Research, v. 97, p. 7791–7797.

Zuber, M.T., Solomon, S.C., Phillips, R.J., Smith, D.E., Tyler, G.L., Aharonson, O., Balmino, G., Banerdt, W.B., Head, J.W., Johnson, C.L., Lemoine, F.G., McGovern, P.J., Neumann, G.A., Rowlands, D.D., and Zhong, S., 2000, Internal structure and early thermal evolution of Mars from Mars Global Surveyor topography and gravity: Science, v. 287, p. 1788–1793.

Manuscript Received 10 August 2007
Revised Manuscript Received 16 February 2008
Manuscript Accepted 14 March 2008

Printed in the USA